THE DEVELOPMENT OF A FAST TIME-SORTER AND ITS USE IN THE MEASUREMENT OF THE LIFETIME OF POSITRONS IN ALUMINIUM AND MICA

by

GARTH JONES

A THESIS SUBMITTED IN PARTIAL FULFILMENT OF
THE REQUIREMENTS FOR THE DEGREE OF
MASTER OF SCIENCE

in the Department
of
PHYSICS

We accept this thesis as conforming to the
standard required from candidates for the
degree of MASTER OF SCIENCE

Members of the Department of Physics

THE UNIVERSITY OF BRITISH COLUMBIA

September, 1955

ABSTRACT

A new type of fast "time-sorter" has been developed, employing a germanium diode as the detecting element. This instrument converts time delays between coincident events into a pulse amplitude distribution, which is then analyzed by a "kick-sorter", enabling a complete coincidence resolution curve to be recorded simultaneously. The resolution curves obtained with this apparatus were found to have half-widths of about 1 milli-microsecond, comparable with those obtained by delayed coincidence circuits.

Using this time-sorter, the lifetimes of positrons in Aluminium and Mica were then studied. The positron life-time in Aluminium was obtained by measuring the centroid shifts between the coincidence resolution curves resulting from the observation of a Na^{22} source embedded in Al, and an assumed "prompt" source of cascade gamma rays, As^{76}. This latter source was employed for the comparison because the energies of its coincident gamma rays are similar to the 1.28 Mev and 511 Kev. gamma rays of Na^{22}. This eliminates the problem of centroid shifts due to inequalities in pulse-height and rise-time between the two sources.

The positron life-time in mica was obtained by comparing the centroid shifts of the resolution curves resulting from the annihilation of positrons in mica and in Aluminium.

The measured positron lifetime in Aluminium is

$$(1.6 \pm 0.4) \times 10^{-10} \text{ sec.},$$

and the lifetime in Mica is longer than this value by

$$(0.7 \pm 0.4) \times 10^{-10} \text{ sec.}$$

ACKNOWLEDGMENTS

I would like to thank my supervisor, Dr. J.B. Warren, for many suggestions during the course of this research, and Dr. C.A. Barnes for helpful discussions during the thesis preparation.

I also wish to thank Mr. G.C. Neilson for many helpful discussions and assistance.

Thanks are also due the other members of the Van de Graaff group, especially Dr. K.L. Erdman, Mr. L.P. Robertson and Mr. J.B. Elliott who offered much in the way of knowledge and assistance.

Finally, I wish to thank the National Research Council for scholarships which have enabled me to carry out these studies.

TABLE OF CONTENTS

TABLE OF CONTENTS - CONTINUED

TABLE OF CONTENTS - CONCLUDED

LIST OF ILLUSTRATIONS

LIST OF ILLUSTRATIONS - CONTINUED

CHAPTER I

INTRODUCTION

Accurate measurements of time intervals of the millimicrosecond range were first made possible by the development of the scintillation counter as a nuclear particle detector (Kallmann 1947, Deutsch 1948) and the application of associated "fast" electronic techniques. The development of this technique was responsible for rapid advances in many fields of nuclear physics, one example being the investigation of the various modes of positron annihilation. This problem is important, since it is a direct experimental method of testing fundamental electrodynamical considerations, such as those which led to the derivation of the Dirac cross-section for annihilation of a moving positron. (Heitler 1954).

The consideration of possible hydrogen-like, bound states of positrons and electrons by Ruark (1945) and Wheeler (1946), led to detailed theoretical investigations of this new "atom","Positronium," by Pirenne (1947) and others (De Benedetti and Corben 1954). The development of devices for measuring very short time intervals enabled workers like Deutsch (1951), and De Benedetti (1954), to detect the existence of this "atom" and measure many of its physical properties.

The measurement of absolute positron lifetimes in various materials was also attempted (Bell and Graham 1953) in order to determine the cross-section for annihilation. Conflicts between the results of the measurements and the original Dirac theory, such as: the existence of two exponential lifetimes in gases and many amorphous substances, and the constancy of the lifetime of positrons in metals, were attributed to the formation of positronium. However, since inconsistencies between the experimental and theoretical data are still evident (Garwin 1953, Dixon and Trainor, 1955), the project of constructing a suitable fast-coincidence apparatus and the measurement of some of these lifetimes was deemed worthwhile.

The object of this work has thus been the construction of a fast-coincidence circuit and an attempt to measure the absolute lifetime of positrons in Aluminium and Mica.

CHAPTER II

THE CONSTRUCTION OF A FAST TIME-SORTER CIRCUIT

1. A Discussion of Previous Fast Coincidence Circuits

A coincidence circuit, as defined by Bell (1954), is: "A nonlinear circuit having two inputs and one output, such that a pulse is delivered from the output only when the two inputs have received pulses within a short time of each other." This short time is termed the resolving time of the coincidence circuit. The definition of resolving time usually is taken as $2\tau_o$, the full width at half height of the prompt coincidence resolution curve, (the measured curve of coincidence counting rate as a function of delay time artificially inserted between the pulses from the two counters). The reduction of this resolving time has thus been the primary objective in the design of these circuits. Bell, Graham and Petch (1952) were the first to construct a coincidence circuit with a resolving time in the millimicro-second range. For 1P21 photomultipliers with stilbene phosphors excited by 100 Kev. electrons, they predicted and observed a minimum resolving time for ninety per cent coincidence efficiency of $2\tau_o = 2 \times 10^{-9}$ sec.

Since 1949, a wide variety of coincidence circuits designed with resolving times in this range have been published.

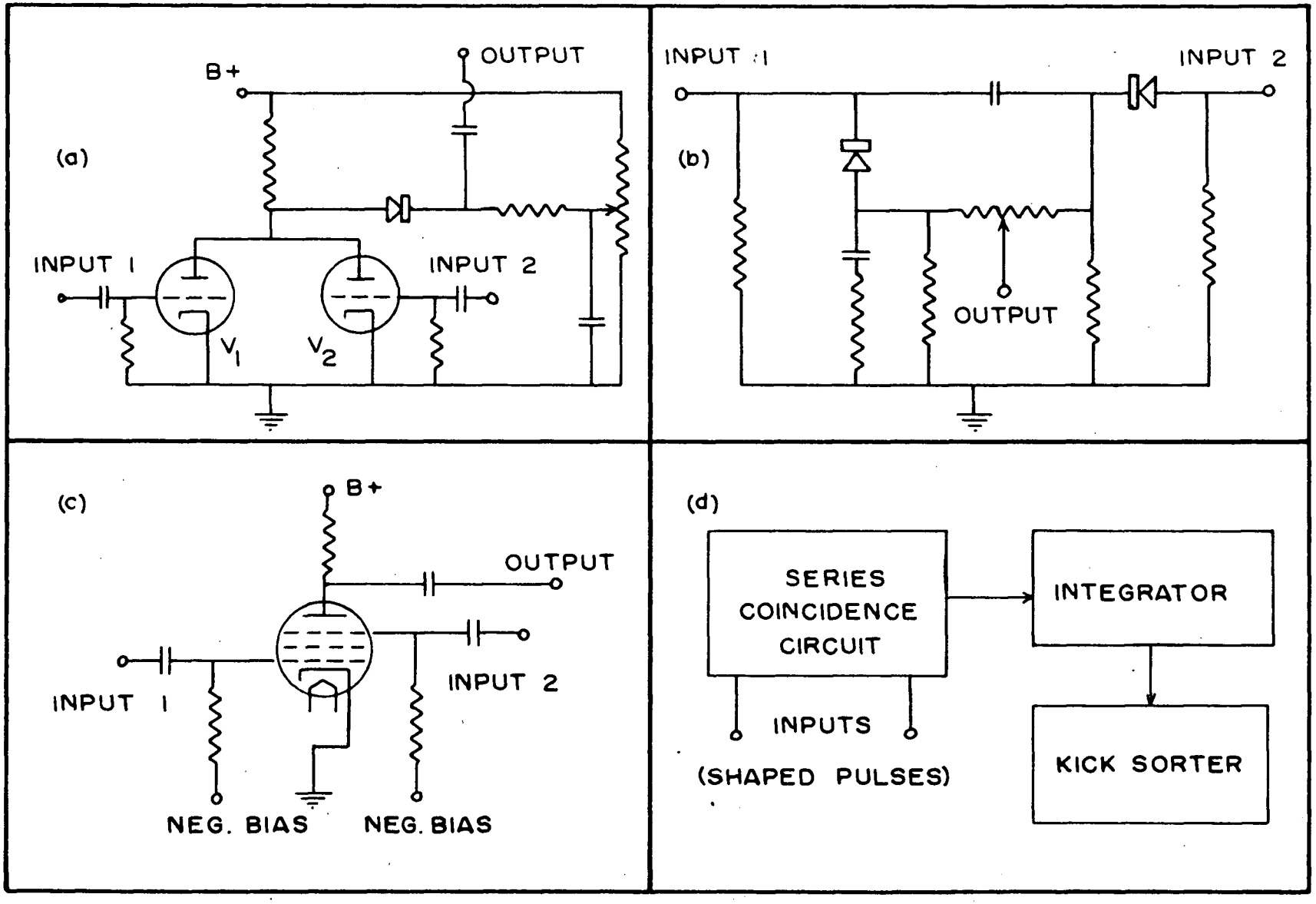

FIGURE 1: (a) PARALLEL COINCIDENCE CIRCUIT
(b) BRIDGE COINCIDENCE CIRCUIT
(c) SERIES COINCIDENCE CIRCUIT
(d) A SERIES TIME-SORTER

These circuits have been classified by Bell (1954) into three types, viz., the parallel, bridge, and series circuits.

A. The Parallel Coincidence Circuit. The first, and one of the most popular of the fast coincidence circuits, is the one mentioned above, designed by Bell, Graham, and Petch (1952), which falls into the "parallel" class, since it is a development of a Rossi, or parallel, coincidence circuit. This type of circuit consists of a pair of pulse size limiters (V_1 and V_2 of Fig. 1_a), an element for adding the equalized pulses (plate load), and an element for detecting pulses of larger than "single" size (diode).

Many such circuits, some with slight modifications of these basic essentials, have been constructed in recent years. However, the original circuit of Bell, et al., (1952), remains one of the best of this type.

B. The Bridge Coincidence Circuit. Another type of coincidence circuit (which first appeared in 1948, Meyer et al.), and which has the obvious advantages of being simple and compact, and requiring relatively small input pulses, is the "bridge" coincidence circuit. This circuit embodies a balanced bridge, usually of germanium diodes, across the diagonal corners of which are applied the two input pulses, with the output pulses being obtained across the other diagonal. The principle of the circuit is that such a bridge may be designed with two "balance" conditions, the first being the normal, static

balance, and the second being an unstable one, reverting back to the first balance state, after a short time (about one microsecond). When a pulse from one counter is applied to the circuit, the circuit is switched into the second balance state described above, with no output pulse produced. The balance of the bridge is upset, however, when both pulses are incident upon the circuit simultaneously, and an output pulse is obtained. As in the other circuits, shaped input pulses are usually employed. A detailed description of the operation of the Bridge circuits is given in the literature. (Bell 1954).

The main disadvantage of this type of coincidence circuit is the difficulty in maintaining the balance of a bridge containing non-linear elements over a wide range of input pulse amplitudes. Thus, large single pulses, will, on occasion, produce a sufficient output pulse to be recorded as a coincidence. This fear of the single pulse effect has apparently hampered the application of this type of circuit to actual coincidence experiments (Bell 1954).

C. The Series Coincidence Circuit. The third type of circuit, the "series" coincidence circuit, was originated by Bothe (1930) in 1930. The basic circuit of this type is illustrated in Fig. (1c), in which a multigrid tube incorporating two control grids is used (such as the 6AS6, or more recently the 6BN6). In this system, both grids are operated at cut-off, so that, effectively, no plate current flows

either in the quiescent state, or when only one of the control grids receives a positive pulse. Only the simultaneous application of positive pulses to both grids will cause anode current to flow. This type of coincidence circuit has the advantages of not requiring equalized pulses, and of possessing a very positive action, since no anode current can flow in the absence of overlapping input pulses. A disadvantage of the circuit lies in the fact that troublesome effects occur when the series coincidence circuit is used at resolving times of the same order as the electron transit time through the tube. Fischer and Marshall (1952), however, have shown that these effects do not destroy the usefulness of the series circuit at these resolving times.

D. Fast Time-Sorters. A useful modification of the series coincidence circuit was developed by Neilson and James (1955), in which a 6BN6 tube is used as a series detector (Fig. 1d). With shaped, rectangular pulses applied to the two grids, the duration of anode current flow is proportional to the overlap in time of the input pulses. When this anode current is integrated by means of a Miller circuit, the amplitude of the output pulse is proportional to the degree of overlap in time of the input pulses. A circuit which performs this type of time-amplitude conversion is termed a "time-sorter."

The time-sorter method of obtaining coincidence resolution curves possesses several advantages over the delayed

coincidence technique. The investigator is able to obtain a complete resolution curve simultaneously, rather than obtaining the measurements point-by-point, with a resultant saving in time by a factor of about fifteen. Because of the shortening of time necessary to obtain the desired curves the results are less sensitive to slow variations in gain and measurements involving weaker sources are made possible. Another advantage is the inherent ability to obtain as many points on the resolution curve as desired, with the upper limit now being set by the number of channels in the kick-sorter rather than by the accuracy say, in resetting a helical delay line to some particular point, as in the circuit of Bell et al. (1952). Perhaps the most attractive characteristic of this technique is the insensitivity of a time-sorter resolution curve to decay of the source. Since the whole curve is obtained simultaneously, no corrections for source decay are required.

Resolving times of the order of 2×10^{-9} sec. have been obtained with the apparatus of Neilson and James (1955). Some speed is lost with their circuit, however, since the 6BN6 requires relatively large input pulses for proper operation, thus necessitating larger plate loads for the limiters and the addition of cathode followers to feed the connecting cable. Both these factors tend to restrict the resolution time obtainable to a value larger than that provided by the parallel coincidence circuit of Bell et al. (1952).

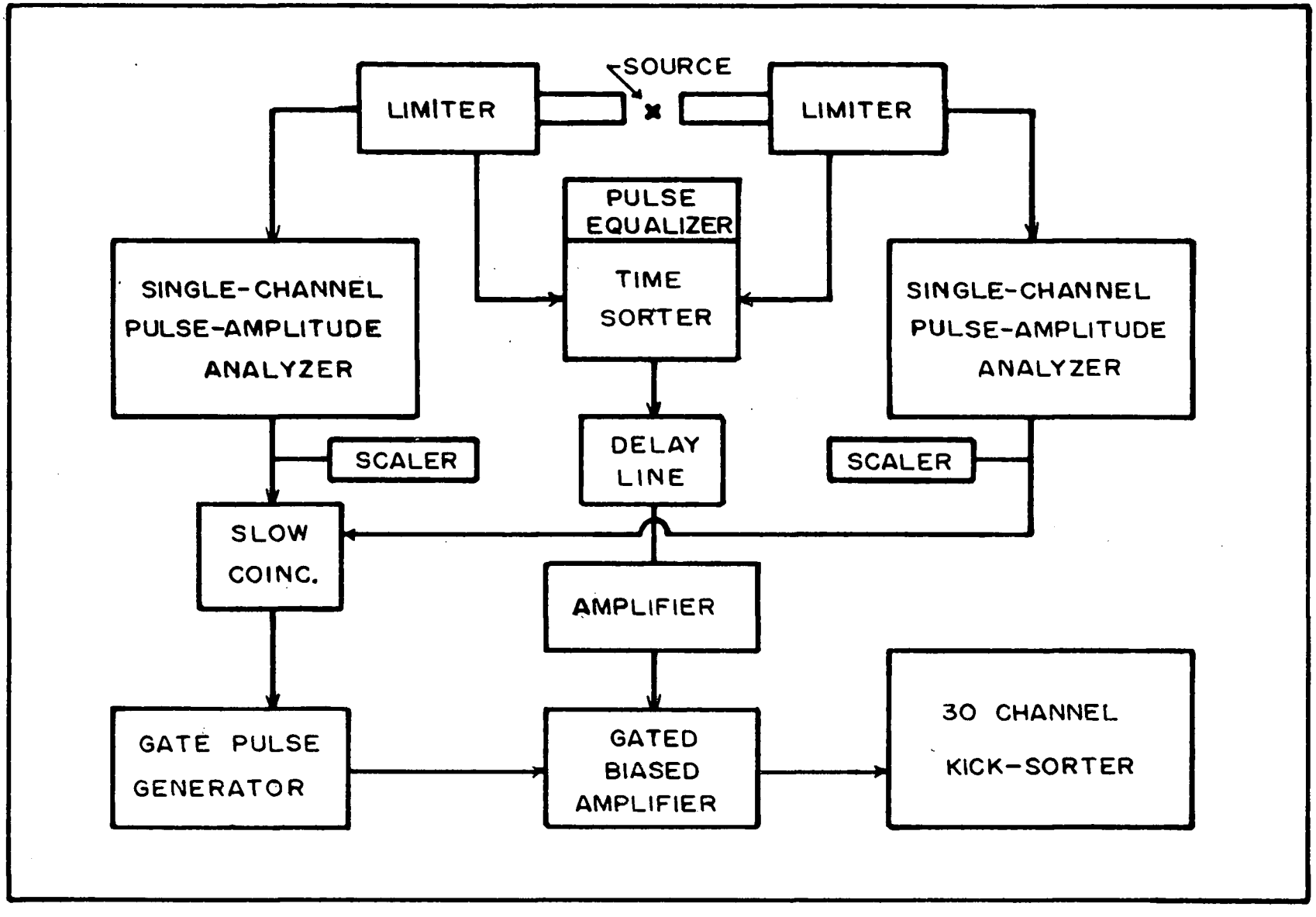

FIGURE 2: BLOCK DIAGRAM OF FAST TIME-SORTER

A New, Fast Time-Sorter. The first part of this thesis describes the development of a "fast" time-sorter circuit of comparable resolution time to the circuit of Bell et al (1952), employing a crystal diode as the non-linear detector, and which has been found useful in measuring time intervals in the 10^{-10} sec. range.

2. Description of the Circuit.

A. Preliminary. Originally, the intention was to construct a fast coincidence circuit of the Bell, Graham, and Petch (1952) type. To this end, a helical delay unit and associated apparatus were constructed. After the apparatus was completed, test runs were made, with the results analyzed to determine the coincidence efficiency and resolving times obtained. (See Appendix A).

Consideration of the method of operation of the unit then suggested that with some alterations of the circuitry, a time-sorter type of operation might be feasible. With this object in mind, work was begun on the circuit described in the following section.

B. Elementary Description of Operation (Block Diagram, Fig. 2)

1. The Counters. The counter, itself, is composed of an organic scintillation phosphor with a very short decay constant, coupled optically to a photomultiplier tube of high gain and short rise time. With a high voltage supply greater

than two thousand volts, this type of counter is capable of producing an output voltage pulse with a rise-time of the order of a millimicrosecond.

ii. The Limiters and Shorting Stub. Since this time-sorter is to analyze degrees of time overlap only, all other variables which would affect the electronic detector, such as pulse amplitude and length, must be normalized and kept constant for all pulses produced by the counters. This action is performed by the limiters and shorting stub. The limiter limits all pulses to an amplitude of about one volt, producing a step function, with a finite rise-time, of a length dependent on the length of the incident pulse. Thus the first part of the normalizing action is accounted for.

The shorting stub is a shorted coaxial cable which serves to clip the incident pulse to a uniform length of about five millimicroseconds. By this means, the equalizing process is completed, and all pulses observed by the detecting diode are uniform in amplitude and length. A slight variation ($\backsim 10^{-10}$ sec) still exists, however, in the rise-time of the rectangular pulses as a result of the variation in amplitude and rise-time of the pulses produced by the counter itself.

iii. The Time-Sorter. The time-sorter consists essentially of a biased germanium diode and a capacitor to ground. If both limiters produce pulses within five millimicroseconds, then by the theorem of the superposition of

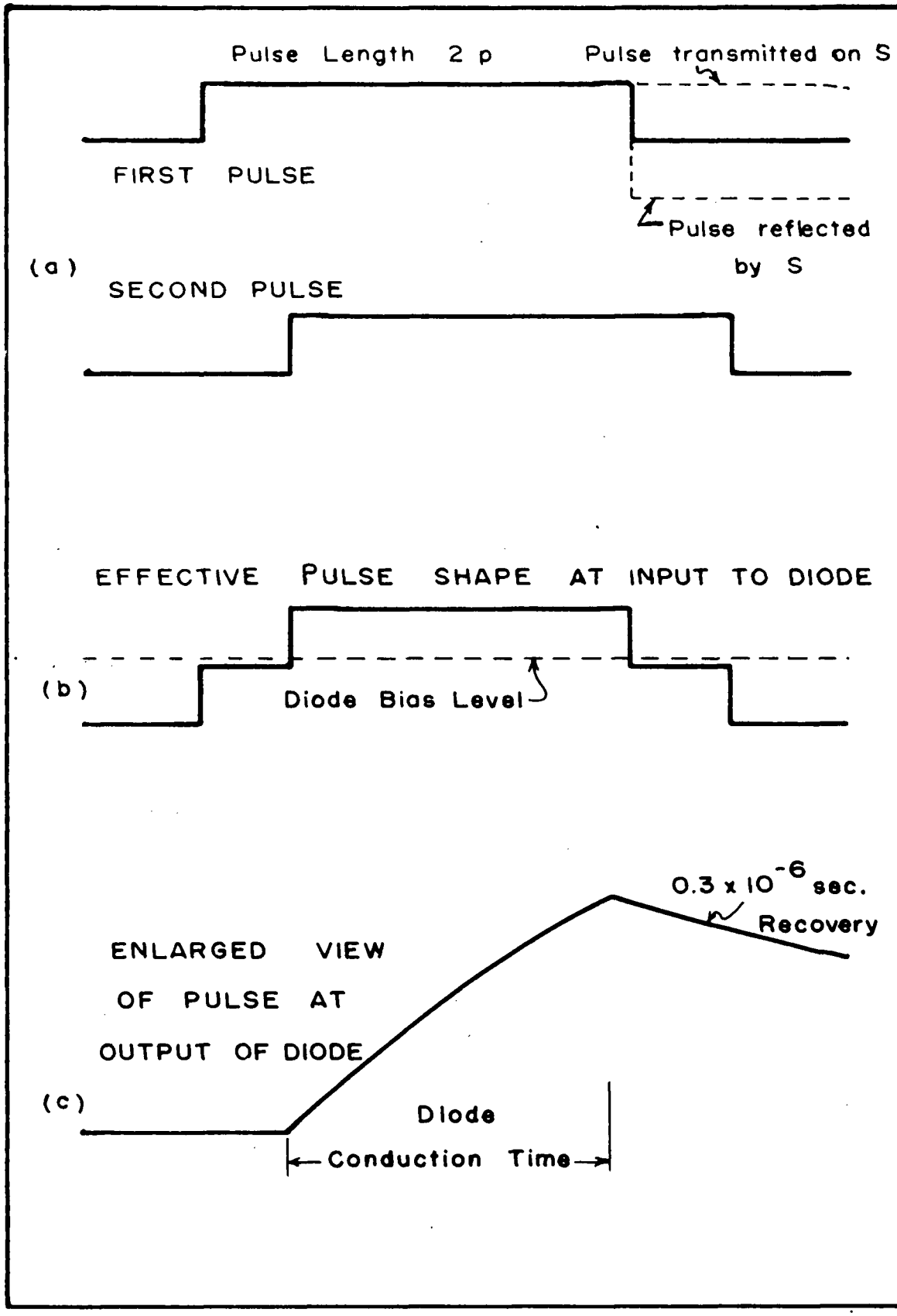

FIGURE 3: METHOD OF TIME-SORTER OPERATION

potentials, there will be a portion of the resulting pulse at the diode input which has an amplitude twice that of the single pulse. With the bias of the diode adjusted to be equal to the amplitude of the single pulses, the diode will conduct only when there is an overlap of the pulses, (see Fig. 3). The current passed by the diode is then integrated by the following capacity to ground, producing a voltage pulse whose amplitude is a function of the overlap in time of the incident pulses.

The diode in the time-sorter also serves as a pulse stretcher, isolating the charge on the condenser from the rest of the circuit when the overlap portion of the incident pulse disappears. Thus, relatively "slow" amplifiers (a bandwidth of about one megacycle/sec.) may be used following the time-sorter.

Time-sorter operation may therefore be obtained by modifications not only of the series coincidence circuit, but also of the parallel coincidence circuit.

iv. The Main Amplifier.* Since the diode actually conducts only a minute quantity of charge, the pulses on the condenser must be amplified before introducing them to the rest of the circuit. This action is performed by the main amplifier.

---

* Linear Amplifier, Type AEP 1444, by N.F.Moody and W.D.Howell, Chalk River, Ontario.

v. The Side-Channel Pulse-Height Analyzers*. Since the amplitude and rise-time of the output pulses of the counters is strongly dependent on the energy expended in the scintillator (Bell et al. 1952), the pulses introduced to the time-sorter are not absolutely uniform in size and shape. To overcome this difficulty, it is necessary to count only those time-sorter output pulses which correspond to counter pulses selected in amplitude, since the output pulse amplitude of the counter is a function of the energy expended by the gamma ray in the crystal. The side-channel, pulse-amplitude analyzers, which accept untreated pulses from the second-to-last dynode of the photomultiplier, perform the task of selecting the counter pulses.

The side channels also enable one to select gamma rays of a specific energy by adjusting the discriminators so that only the voltage pulses corresponding to that energy are selected. A square negative pulse of one microsecond duration is produced by the analyzers when the input pulse amplitude lies within the preset bias levels.

vi. Slow Coincidence Unit and Gate Pulse Generator. The outputs of the side channels are connected to a slow ($\sim 1\,\mu$sec.) coincidence unit which then produces a square, negative pulse when both side channel analyzers have received acceptable

---

* Pulse Amplitude Analyzer, Designed by R.E.Bell and R.L. Graham. A.E.C.L., Chalk River, Ontario

pulses within a resolution time of about one microsecond. These pulses, when incident upon the Gate Pulse Generator, trigger a univibrator, which in turn produces the large (30 v.), positive pulses needed to operate the "gate" of the biased-amplifier.

vii. The Gated Biased-Amplifier. The gated biased-amplifier amplifies those input pulses from the fast, centre channel, which have an amplitude greater than an adjustable bias voltage. These amplified pulses are then released to the 30 channel, Marconi Kick-sorter* whenever the "gate" is activated by the gate-pulse generator, thus ensuring that the pulses counted by the Kick-sorter do correspond to the selected counter pulses.

In order for the biased-amplifier to receive the positive gate pulses and the time-sorter pulses in coincidence, it is necessary to insert a delay line of about 1½ micro-seconds between the time sorter and the Moody linear amplifier to correct for the natural delays inherent in the side channel equipment and gate pulse generator.

C. A Detailed Desciption of the Components and Associated Problems.

i. The Counters. The ultimate limitation imposed on the resolving time of coincidence circuits is due to the un-

---

* Pulse Amplitude Analyzer (Kicksorter); Marconi Type #115-935

certainty in the time of ejection of the first photoelectron from the photocathode after the excitation of the phosphor by the particle being counted. (Bell et al. 1952). Post and Schiff (1950), by considering the phosphor, optical coupling, and photo-cathode as a unit, derived the following expression for the mean time delay for the appearance of the first photoelectron: $\bar{t} = \frac{\tau}{R}\left(1+\frac{1}{R}\right)$, $(R>>1)$.
where τ is the mean life of the light flash from the phosphor, and R is the total number of photo-electrons produced during the pulse.

Thus, the desirable features of the scintillator are that the scintillations be intense (large R) and of short duration (small τ). Diphenylacetylene was chosen for the scintillator in preference to stilbene, since the manufacturer* supplies the following data concerning these crystals.

Material	Relative Light Yield to Betas	Decay Constant (x 10^{-9} sec.)
Stilbene	0.65	8
Diphenylacetylene	0.8	4

The choice of the photomultiplier tube then depends on obtaining high gain and a short rise time (in response to a square pulse), ensuring that the spread in electron transit time is small. To date, the RCA 1P21 is the only commercially

---

* National Radiac Inc., 10 Crawford St., Newark 2, N.J. Bulletin #5.

available tube which combines a high gain with short rise time as indicated by the following table taken from Bell (1954).

Photomultiplier	Dynode Structure	Gain (10^6)	Rise Time ($\times 10^{-9}$ sec)
RCA 1P21	931A	about 100 (2000 v)	1
RCA 5819	Large Cathode + 931A	0.6	5
RCA 6342	Large Cathode + 931A	0.6	5
RCA H4646	Curved dynodes in line	1000	2
EMI 5311	Venetian Blind	10	7
Du Mont 6292	Quarter-circle boxes	1	about 10

When the 1P21 is operated in excess of 2000 volts, Bell et al. (1952), have shown that the gain is about 2×10^8 since one photo-electron will produce an output pulse of the order of 3 volts across 10 pf. They have also indicated that at these voltages, the transit-time spread is not a serious effect for resolving times of the order of 10^{-9} sec. Although the 1P21 photomultiplier is designed for a voltage of 1200 volts, most will operate at the higher voltages without breaking down if the high voltage is applied gradually over a period of about a day. At voltages in excess of 2000 volts, however, noise and spurious pulses are found to increase tremendously. A close-fitting conducting shield seems to be effective in decreasing the noise intensity somewhat. (Mackenzie 1953). This shield is insulated from the rest of the circuit &

and allowed to float to the H.T. potential. Of the tubes used, one was silvered over the surface of the tube, with the exception of the photo-cathode window, and the other was wrapped with .001 inch aluminium sheet. Since even with this added protection, the noise in one of the tubes became excessive at voltages greater than about 2200 volts, this value was used as the photomultiplier supply voltage in the subsequent experiments.

a. The Counter Assembly. Since the manufacture of the 1P21 phototubes was found to be inconsistent as far as physical size and alignment is concerned, a solid crystal mount (as described by Mackenzie 1953) was found unsuitable. The following method of mounting the crystals was used in the equipment and found to be quite satisfactory.

The diphenylacetylene crystal was 1 in. x 3/8 in. x 3/8 in., with one longitudinal face being machined by the manufacturer to fit the side of a 1P21 phototube (i.e. an arc of 19/32 in. radius). This crystal was then placed in a small cardboard box with MgO packing around the sides. Optical coupling between the crystal and the phototube was provided by a film of 10^6 centistoke oil. To insure a firm contact between the crystal and the glass, several rubber bands were wrapped around the crystal mount and tube. The whole mount was then well covered with black scotch tape to prevent light leaks.

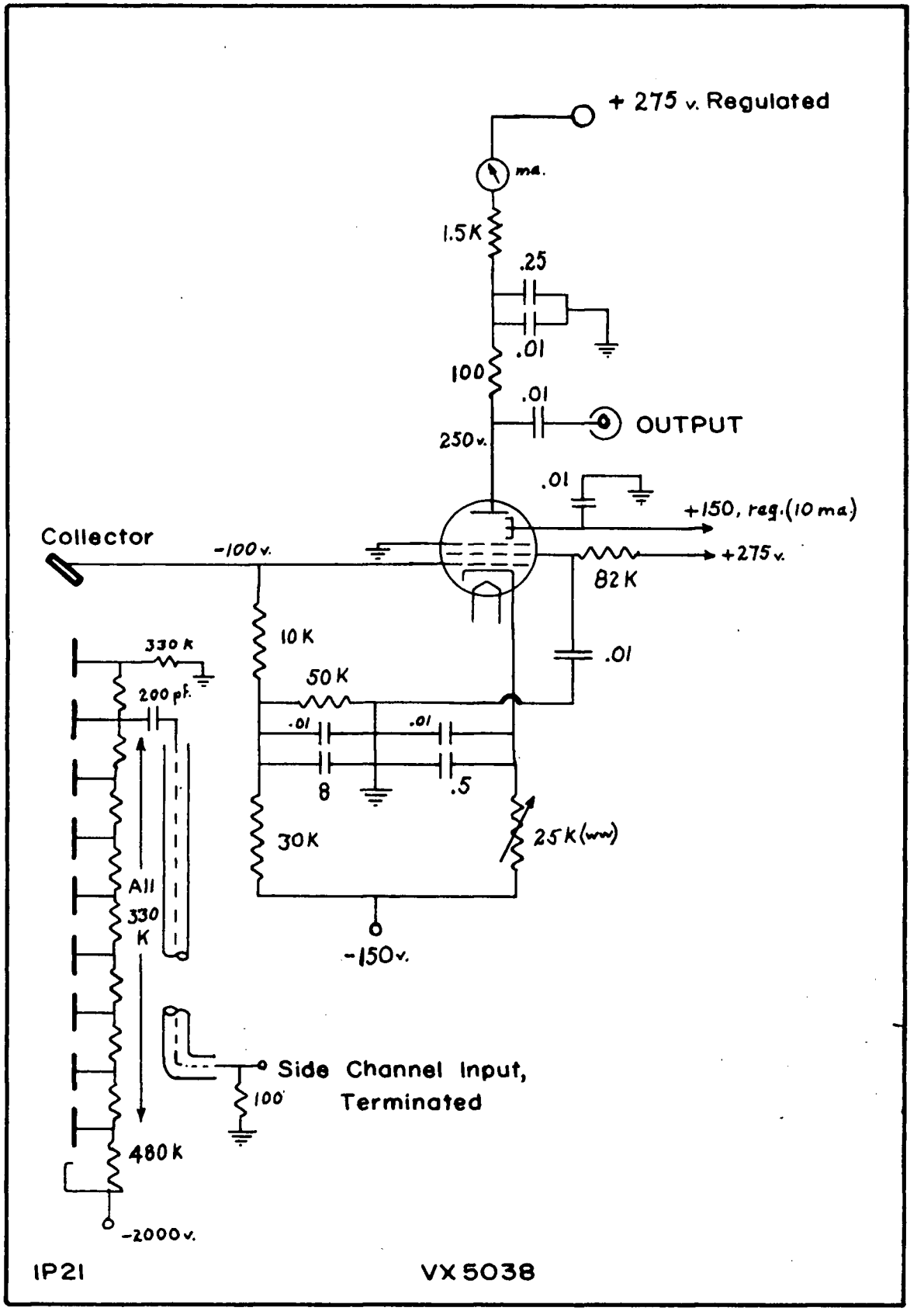

FIGURE 4: LIMITER CIRCUIT

b. Voltage Supply and Socket Considerations. The use of black, cloth-filled bakelite sockets for the photomultiplier tubes was found to be highly unsatisfactory, since large spurious pulses were observed on the output pin at voltages in excess of 1500 volts, the amplitude and frequency increasing with increasing voltage. These pulses were present without the tube inserted in the socket and were believed to be associated with water adsorption on the surface of the bakelite, since washing with pure ethyl alcohol eliminated this condition for about ten to fifteen minutes. Then, however, the noise would gradually recur. The use of brown, mica-filled bakelite sockets essentially eliminated this problem, as they produced very few of these spurious pulses at the voltages employed.

The socket wiring is shown in Fig. 4. With the bleeder-chain values indicated, the following potentials were obtained; 190 volts between dynodes, 90 volts between the dynode and collector, (kept lower than the dynode-dynode potentials for reasons of stability -- see RCA Tube Handbook), and 270 volts between the dynode and cathode (larger than the dynode-dynode voltage to reduce electron transit-times).

c. Degeneracy of Output Pulses. The fact that the final dynode produces fast positive pulses during operation, of about the same amplitude as the negative, collector pulse, introduces the possibility of degeneration of the negative output pulse, by capacitive coupling between the final dynodes

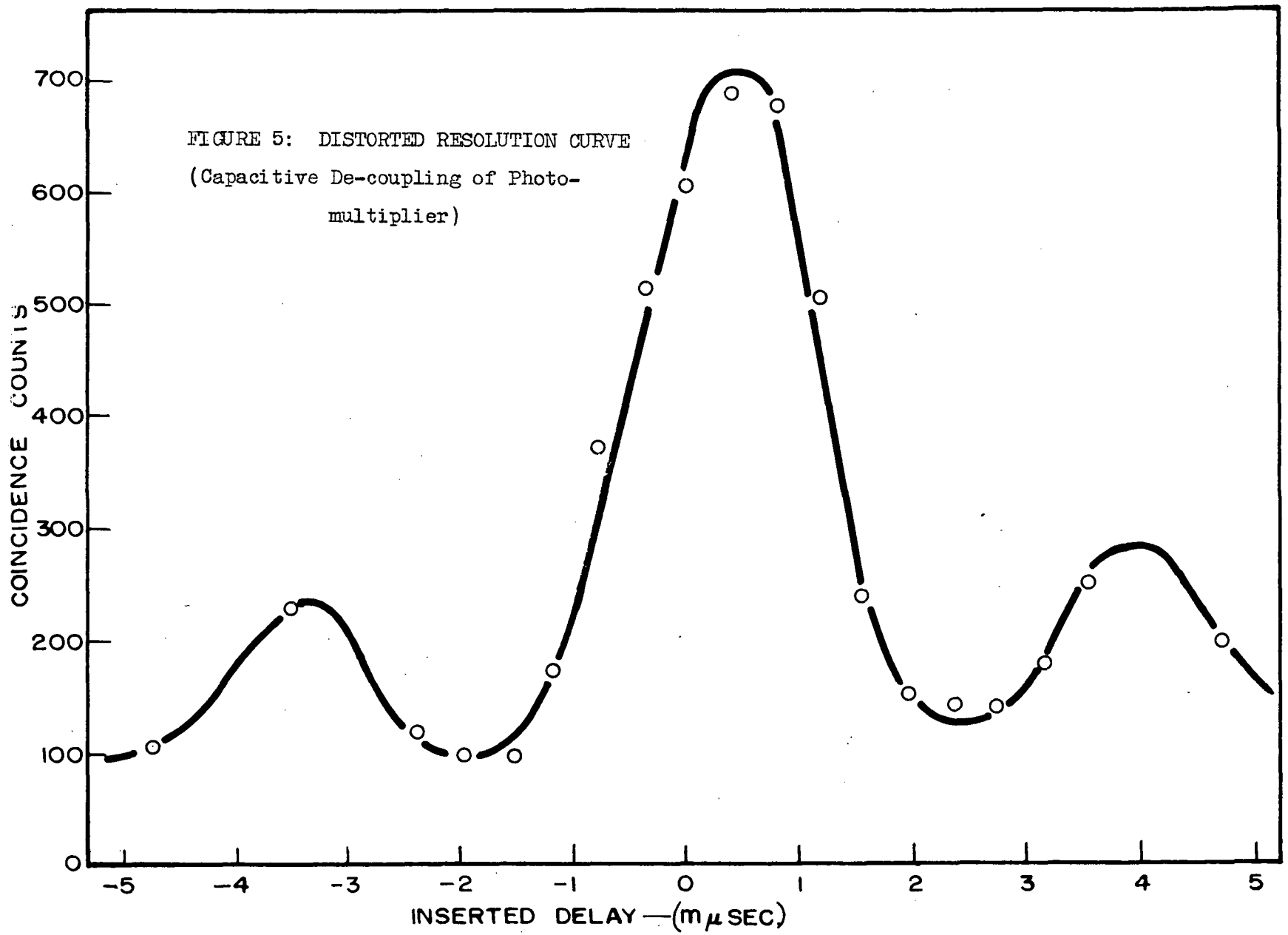

FIGURE 5: DISTORTED RESOLUTION CURVE
(Capacitive De-coupling of Photo-multiplier)

and the anode. For this reason, the possibility of high-frequency by-passing by means of small ceramic capacitors to ground from the last two dynodes was investigated.

The results were quite unsatisfactory, however, since extra peaks were introduced in the coincidence resolution curves. (see Fig. 5). It is believed that the effective short circuit to ground through the ceramic capacitors completed a series resonant circuit between the inductance of the dynode lead wire and the inter-dynode capacities. Damped oscillations of this circuit would superimpose a "ring" on the main pulse, permitting the possibility of its being detected as two or more pulses rather than just one. A rough calculation seems to support this view.

Inductance of straight wire (#22); about 1/40 μh/in. In the case of a 1P21, the dynode lead is about 2 in. long leading to an inductance of 1/20 μh.
The capacity between the last dynode and the other dynodes and anode is about 10 pf. (RCA Tube Handbook).

$$\therefore \omega = \frac{1}{\sqrt{LC}} \simeq 1.4 \times 10^{+9} \text{ rad./sec.}$$

and the time per cycle, is then $2\pi \times 7 \times 10^{-10}$ sec. $\approx$ 4.3 mμ. sec., which is close to the separation time of the peaks.

After these investigations, the photo-tube bleeder chain was returned to the form as shown in Fig. 4: Since the inter-dynode capacities are about 4 pf., it is believed that the last dynode is effectively shunted to earth via the 100 ohm

load of the eighth dynode, as far as the high frequencies involved are concerned.

ii. The Limiters. As mentioned previously, the purpose of the limiters is to produce voltage pulses of uniform amplitude, independent of the amplitude of the input pulses.

a. Choice of the Limiter Tube. The choice of the limiter tube was governed by the following requirements.

As is shown in Fig. 4, the plate load of the limiter consists of a 100 ohm, Telcon AS48 cable in parallel with a 100 ohm terminating resistor. As a result, to be able to produce one volt limit pulses at the anode, about twenty ma. of current must be cut-off in the limiter tube. Thus, one requirement of the limiter is that it be capable of withstanding the plate dissipation demanded.

Since under normal operation, the negative pulse applied to the grid of the tube is at least an order of magnitude larger than the anode limit pulse, a low grid-anode capacity is necessary to preserve the fast wave front of the limit pulse.

Also, in order to retain as many high-frequency components as possible in the output pulse, a very low time constant per unit gain is desired. It is well known that secondary-emission pentodes are much superior to conventional pentodes in this respect. (Bell 1954).

For these reasons, the tube chosen for the limiter was the VX 5038, which possesses the following characteristics.

Since the manufacturer* of the VX 5038 states under "typical operating data" for this tube, a plate current of 15 ma. at 350 volts, the current-handling requirement is satisfied.

Secondly, the grid-anode capacity is: 0.008 pf., a factor of three or four better than conventional pentodes.

Also, with a transconductance of 21 ma/volt (at 20 ma. anode current), the time-constant per unit gain, C_T/g_m (where C_T is the grid-anode capacity, and g_m is the transconductance; Bell 1954), is 6.2×10^{-10} sec., one of the lowest of commercially-available tubes. Thus, with gains of less than one-tenth in the limiter, there should be no loss of speed at this point, the time-constant of the limiter being much less than the time-constant of the input pulse.

b. Discussion of Circuit Operation and Component Values

The occurrence of satellite pulses following the main pulse in the 1P21 has been fully described in the literature (see Mackenzie 1953). To prevent the possibility of separate limit pulses being formed for each satellite pulse, the grid-circuit time-constant must be sufficiently long compared to the satellite spacing that the tube remains cut-off while the satellites are occurring. In the limiter circuit of Fig. 4, the stray capacity to ground of about fifteen pf. for the collector-grid circuit, yields a time-constant of 0.15 microseconds.

* E.M.I. Research Laboratories Ltd., Hayes, Middlesex, England.

Since the satelite spacing is of the order of 0.1 micro-seconds (Mackenzie 1953), this time-constant is sufficiently large.

One difficulty associated with secondary emission pentodes, however, is the large fluctuations in gain to which they are subject. These fluctuations were considerably reduced by the use of a large, variable cathode resistor (25K), which causes cathode follower action as far as d.c. is concerned. When the circuit was in operation, this variable resistor was adjusted so that the limiter produced one volt limit pulses. Stabilization of the quiescent-state operation of the secondary emission pentode was also improved by allowing the tube to warm up at the desired operating point for several days before using. Voltage stabilization was ensured by using regulated d.c. power supplies*, fed by regulated 110 volt a.c.** When this procedure was followed, stabilization over short and long periods was quite satisfactory.

For good high-frequency decoupling in the limiter, ceramic capacitors with short leads were used, and a copper chassis with point-to-point wiring was employed. The suppressor grid and internal shield were grounded directly to the copper chassis as suggested by Mackenzie (1953).

---

* Regulated Power Supply, Model 28, Lambda Electronics Corp., Corona, N.Y.

** Sorenson Regulator, Model 500, Sorenson and Co. Inc., Stamford, Conn.

iii. The Helical Delay Line. As mentioned previously, a helical delay line was constructed according to Chalk River specifications. This part of the equipment was actually unnecessary for the time-sorter circuit but was retained since it facilitated the production of time calibrations, as it was a method of introducing variable delays without introducing impedance discontinuities. The centre conductor, #12 B&S hard-drawn copper wire, was wound onto the brass helix using lucite spacers for positioning. The final diameter of this conductor was 4 7/16 in., with two full turns/inch. Thus, when the helix is rotated one turn, the relative delay between the two channels is changed by two turns (or 2.36 millimicroseconds).

Connection was made to the helix by means of short pieces of 100 ohm cable mounted inside the helix drum, which in turn were connected to the stationary end-plates by means of frictional contacts situated within the helix bearings. Connection to the limiter cables was made by employing fifty ohm Amphenol connectors. Although this represents an impedance discontinuity, the path length is sufficiently short, that a transmission of about ninety per cent is obtained (Appendix B).

iv. The Pulse Length Equalizer. The pulse length equalization was obtained by the use of a shorted coaxial cable, in which a voltage pulse undergoes reflection at the

short circuit, the reflected pulse being out of phase, or of opposite polarity, to the incident pulse.

A pulse from the limiter, upon meeting the junction of the shorting stub and helix sees an impedance discontinuity and suffers a reflection, the resultant pulse height at the junction being $\frac{2Z_s}{Z_o+2Z_s}$ smaller (Mackenzie 1953), where Z_s is the characteristic impedance of the shorting stub, and Z_o is the characteristic impedance of the helix. Since these pulses have a smaller amplitude than the crystal diode bias, the loading effect of the detector will be negligible. However, during pulse overlap, the diode is in a conducting state, with a resultant impedance of about 600 to 100 ohms. Thus an accurate description of the pulse formation during overlap is made difficult by the variable nature of the diode resistance, a strong function of the pulse amplitude, itself.

Although a shorting stub of characteristic impedance equal to 1/2 Z_o should be used to prevent the occurrence of multiple reflections in the shorting stub, it was found, experimentally, that the use of a 100 ohm stub increased the pulse size (an increase of Z_s in $\frac{2Z_s}{Z_o+2Z_s}$) and did not alter the form of the resolution curves. For this reason, a 100 ohm shorting stub was used in the final circuit. The duration of the voltage pulse formed is equal to (twice the cable length) ÷ (the velocity of propagation of the pulse). As far as the operation of the circuit is concerned, the actual length of the shorting stub is immaterial, provided that it is suffic-

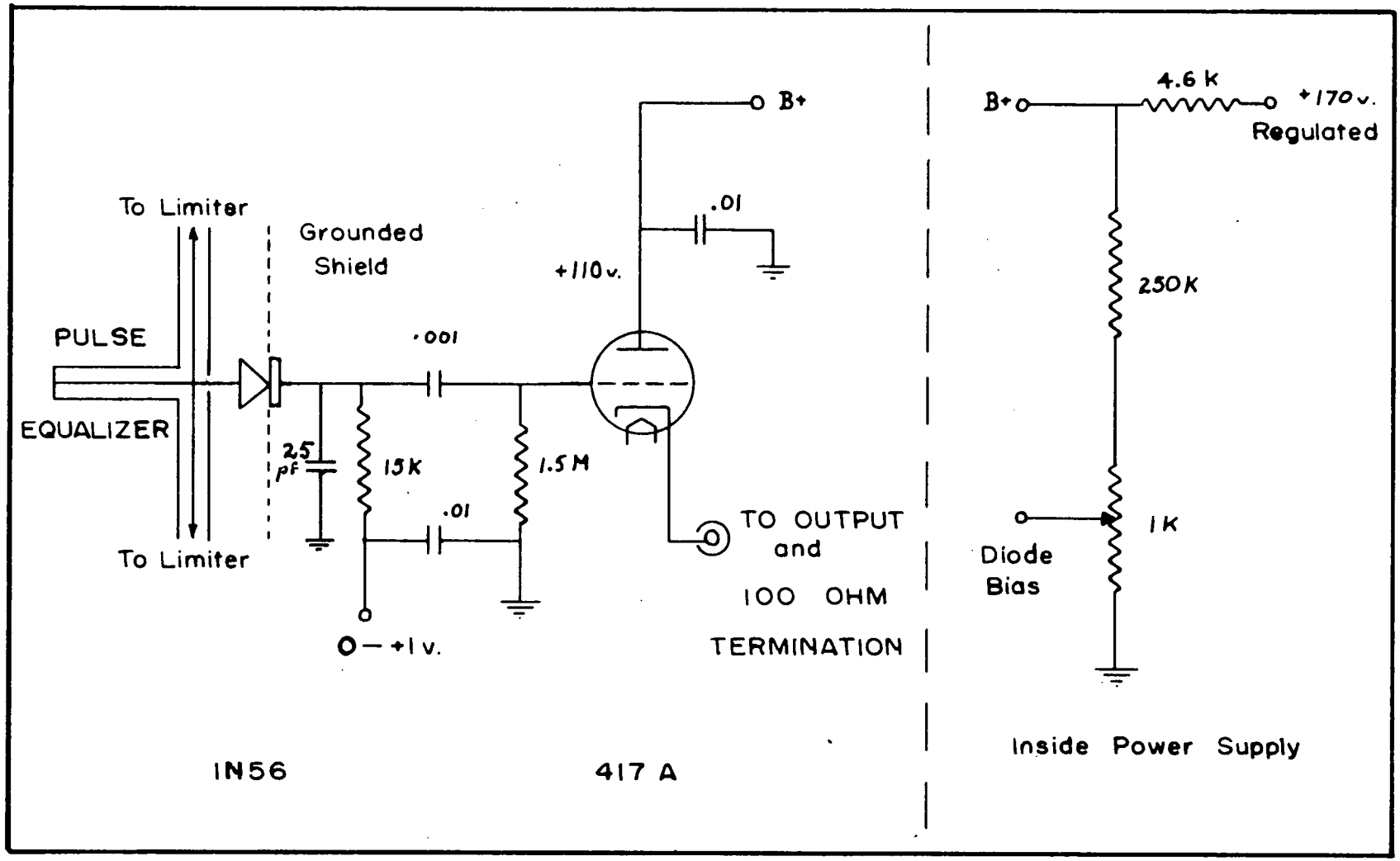

FIGURE 6: TIME-SORTER CIRCUIT

iently long for 100% coincidence efficiency to be realized. It is obvious, also, that when measuring small lifetimes, the change in the degree of overlap will be equal to a few x 10^{-10} sec. In order for this change to be an appreciable fraction of the total conducted pulse, very large overlaps (about 10^{-8} sec.) for the prompt curve are undesirable. Since the coaxial cables have a finite attenuation factor at the frequencies involved, long shorting stubs will have poorer pulse length equalization (more pulse shape distortion), than shorter ones.

As a result, an equalizing stub length of about five millimicroseconds was adopted for the apparatus and was believed to be a reasonable compromise. Variations of this length by a factor of two, however, did not seem to produce any significant differences in the coincidence resolution curves obtained.

Sufficient delay was inserted in one side of the coincidence system to produce an overlap of about 1/2 for prompt pulses. Since the pulse length was 5.1 millimicroseconds, this delay amounted to about one turn from the electrical centre of the helix (equivalent to about 2.3 millimicroseconds of inserted delay).

v. <u>The Time-Sorter</u>. The complete diagram of the time-sorter circuit is shown in Fig. 6.

a. <u>The Diode and Integrator.</u> The equivalent circuit of the diode and grid circuit of the cathode follower is the following:

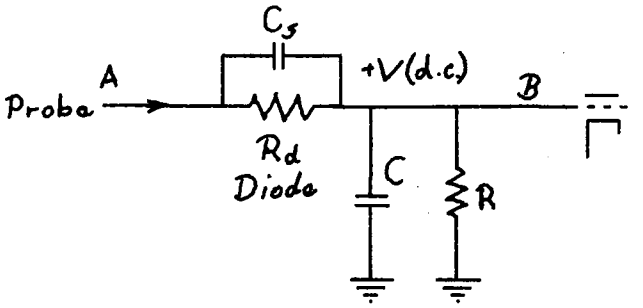

A grounded shield was placed around the diode to decrease the shunt capacity.

R_d is the resistance of the diode, varying from about 500K at -11 volts, through 30K at -0.3 volts, 20K at +0.1 volts to about 63 ohms at 0.8 volts.

C_s is the shunt capacitance; about one pf.

C is the integrating capacitor: 25 pf. + stray and input capacity $\lesssim$ 35 pf.

R is the dc. bias supply resistor of 15 K.

b. <u>The Output Pulse Formation.</u> In considering the various output pulses, we may distinguish several possible cases:

For no overlap, (hence, R_d about 25 K), the pulse visible at B is equal to $C_s/C_{total} = 1/35$ of the amplitude of the pulse at A.

For no overlap, but for the case where the pulses occur within the integration time of the following amplifier,

the pulse obtained is twice as large as in the preceding example.

In both cases, however, the output pulse is obtained by the voltage divider action of the two capacities in series. Thus the length of the pulse will be the same as the input pulse (no pulse-stretching will occur). These pulses, therefore, when incident upon the relatively long integration time constant of the following amplifier (about 0.5 μsec.), will appear many times smaller than the factor of 1/35 given here.

In cases of overlap, R_d is of the order of 500 ohms, with the result that charge is conducted onto C. This charge then decays with the time constant $RC = 15 \times 10^3 \times 25 \times 10^{-12} = 375 \times 10^{-9} \approx 1/3$ microseconds. The integrating capacitor C charges up with the time-constant set by $R_dC = 500 \times 35 \times 10^{-12} = 17.5$ millimicroseconds. The crystal diode used was the type 1N56, chosen for its high conduction characteristics.

Although a larger value of the resistor, R, would have the advantageous effect of increasing the pulse length, most stable results are obtained when R is less than the non-conducting R_d (Lewis and Wells 1954). Since the back resistance of the germanium diode is extremely temperature dependent, a more constant bias voltage is obtained with R much less than Rd, due to the voltage divider action of the two resistors.

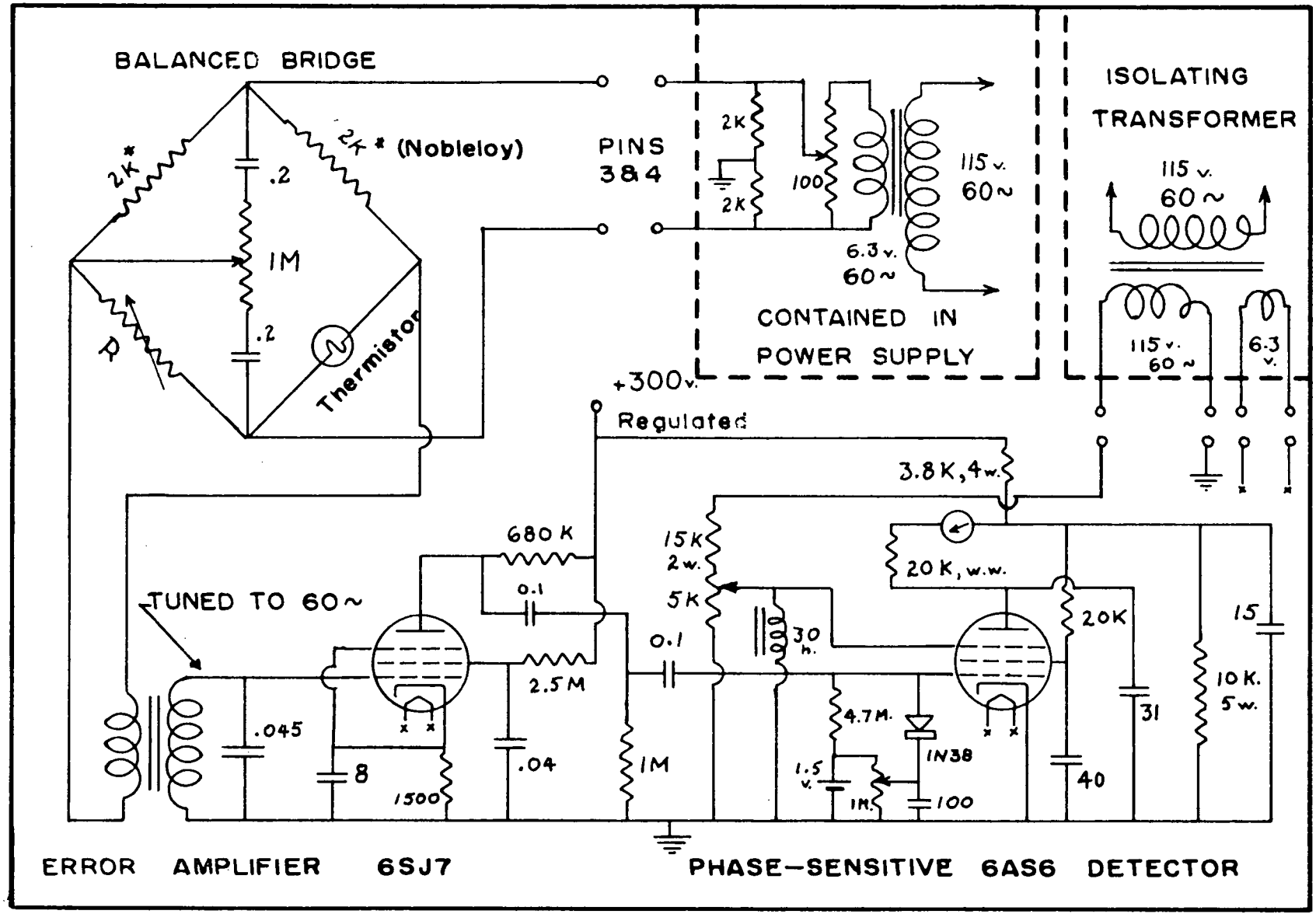

FIGURE 7: TEMPERATURE STABILIZER CIRCUIT

b. The Cathode Follower. As far as the cathode follower is concerned, the tube Western Electric type 417 A was chosen because of its high g_m; its output cable termination was used as the dc. cathode load to keep the heat-dissipating components in the time-sorter chassis to a minimum.

vi. The Temperature Stabilizer. In preliminary runs with the apparatus as described above, shifts of the peak covering up to six channels were noticed on the kicksorter. These shifts were ascribed to resistance changes of the germanium diode following small changes in room temperature, since the diode was by far the most sensitive component of the apparatus. The published data* on the 1N56 diode gives as the variations of static characteristics with temperature:

a variation of about 0.079 ma., or 1/2% of the forward conduction current at an applied voltage of 0.8 volts for a change in temperature of one degree Centigrade, and,

a variation of about 2 μamperes in 10 μamperes of the reverse current for a change in temperature of one degree Centigrade.

For these reasons the temperature stabilizer of Fig. 7 was constructed. A continuously-operating stabilizer was desired in preference to a simpler discontinuous type because of the diode sensitivity to temperature variations. A modification of Benedict's "A.C. Bridge for Temperature Control"

---

* Sylvania Crystal Diodes, Slyvania Electric Products Inc. 1740 Broadway, N.Y. 19, N.Y.

(1937) was employed since it is a relatively simple, yet sensitive instrument.

A Western Electric D164699 Thermistor was used as the temperature-sensitive detector, employed as the sensitive element of a Wheatstone bridge. Variations in its impedance cause a corresponding variation in the amplitude of the output signal with a 180° change in phase when the thermistor impedance passes through the balance point. This signal is then amplified by means of a one-stage audio amplifier of gain 280, whose grid circuit is tuned to 60 cycles with a Q of about 2. The output of the amplifier is then fed into a phase-sensitive detector which compares the phase and amplitude of the error signal with the standard mains a.c. The operation of the circuit is essentially the same as that described by Benedict except for the phase-sensitive detector. As suggested in the original article, a thyratron (in this case, a type 2D21) was first tried as the phase-sensitive detector, with the phase-sensing reference signal applied to the plate and the error signal to the grid. The output current then passed through a 1K heater, also situated in the time sorter chassis. The temperature stabilization of this circuit was very good with temperature stabilities within 0.05°C. obtained over the course of a day and stabilities within 0.1°C. over several days. However, the discontinuous mode of operation of the thyratron inserted radio-frequency hash into the coincidence circuit.

At the expense of some sensitivity, the use of a 6AS6 tube as the phase detector (as shown in the diagram) eliminated this difficulty. In this case, the heater current is well-filtered by by-passing the a.c. component of the plate current to ground. The value of the wire-wound resistor used as a heater had to be increased to 20^{K}, though, because of the lower anode current obtainable with this type of tube. A diode is employed in the grid circuit of the phase-sensitive detector to prevent the drawing of grid current on the positive half cycles of the error signal. The anode current meter reads about 25 ma. full scale.

The stability of the time-sorter was greatly improved by using this device, although greater sensitivity, obtained by adding another stage of audio amplification, might be advisable.

To prevent any variation of the diode temperature due to gross room-temperature fluctuations and draughts, the whole time-sorter apparatus (including the helical variable delay line) was enclosed in a polystyrene** box, to which was added an air mixer and thermostat*, used in conjunction with a 60 watt light-bulb heater, for increased temperature stabilization. The resulting stability of the circuit under these conditions is described in the section on performance.

---

* Thermoswitch, Catalog No. 17500-4/6, Fenwal Inc., Ashland, Mass., U.S.A.

** Styrofoam

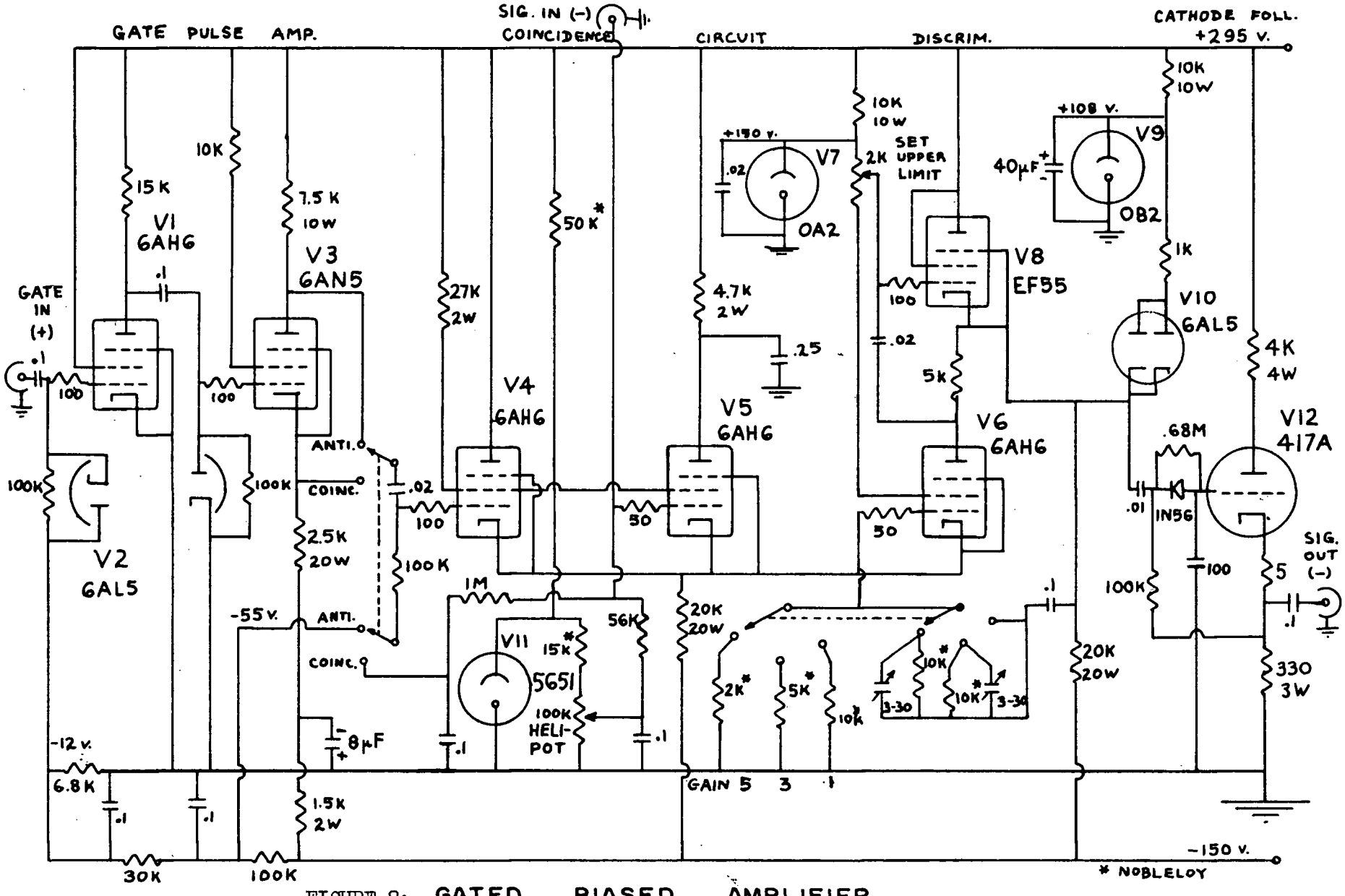

FIGURE 8: GATED BIASED AMPLIFIER

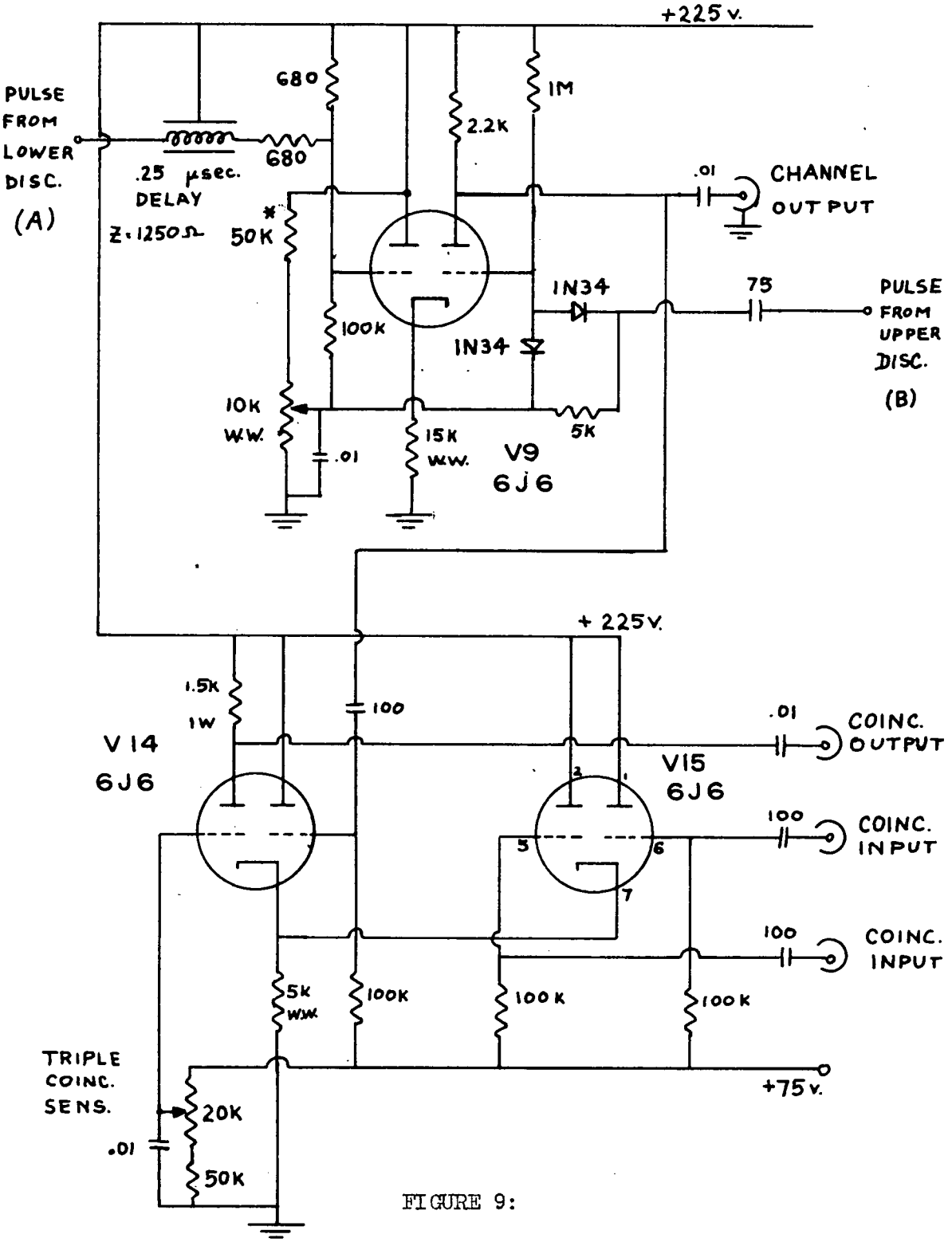

FIGURE 9:

PULSE AMPLITUDE ANALYSER — ANTICOINCIDENCE AND TRIPLE COINCIDENCE CIRCUITS

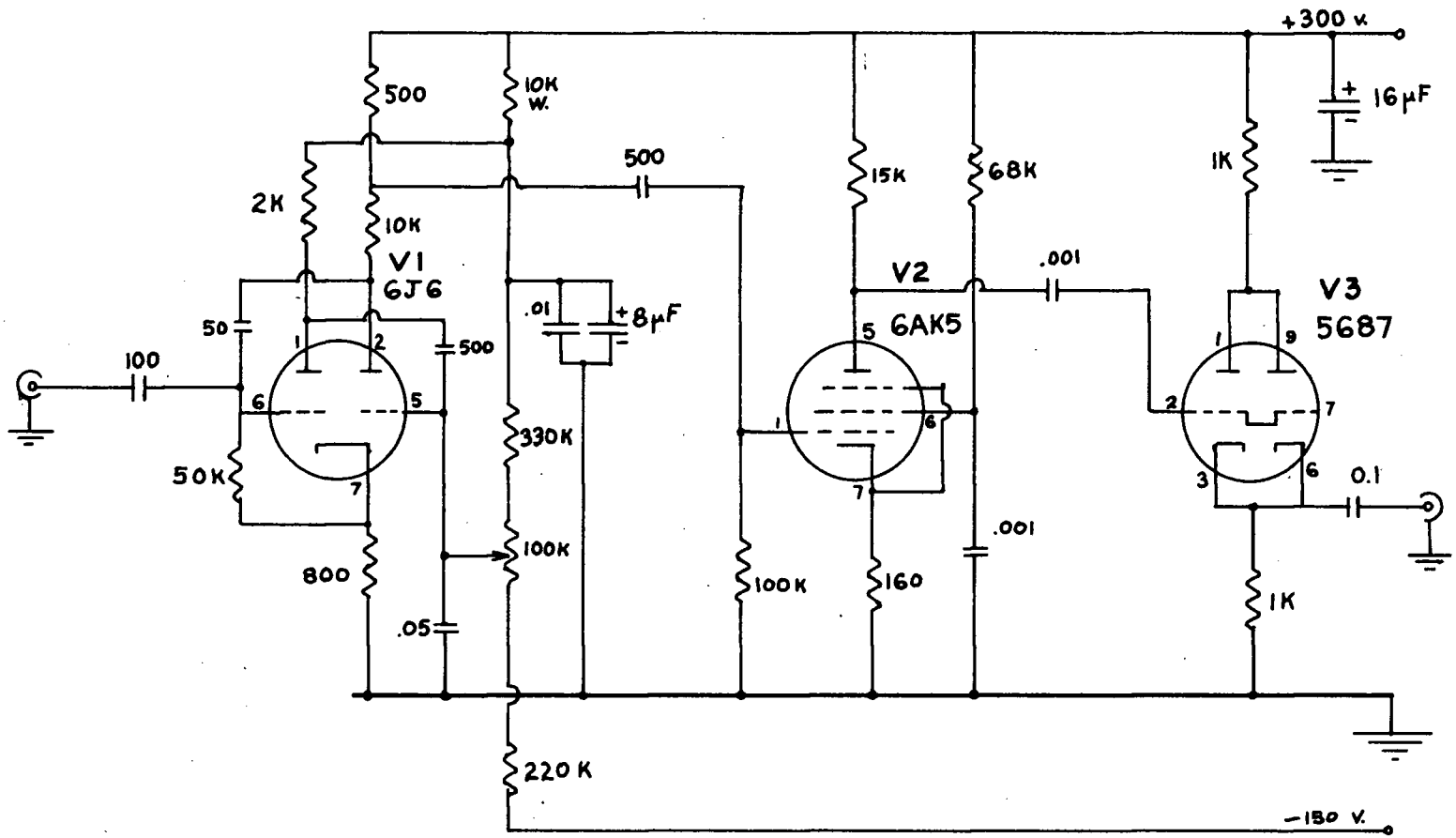

FIGURE 10:

GATE PULSE GENERATOR

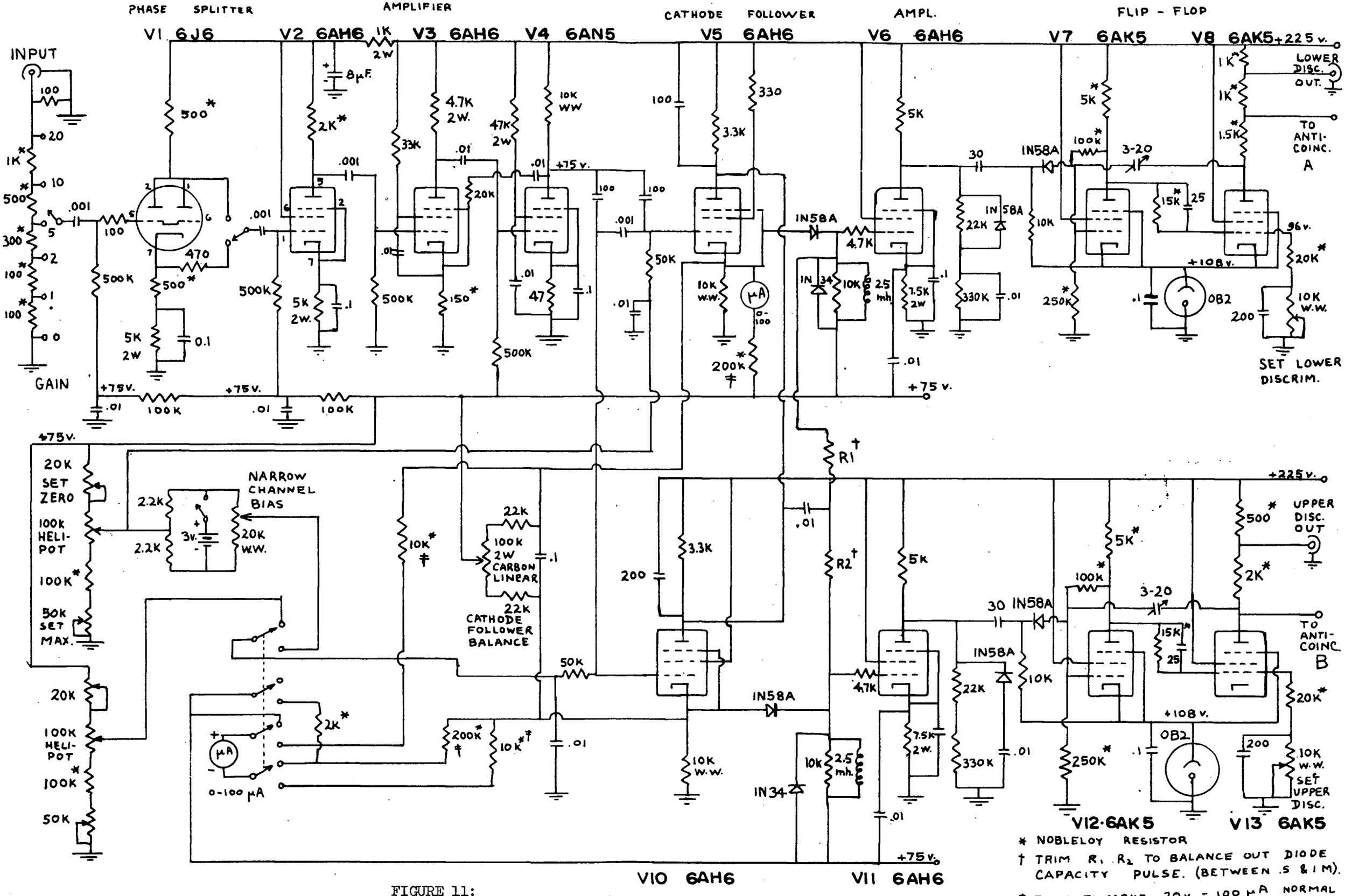

* NOBLELOY RESISTOR

† TRIM R_1, R_2 TO BALANCE OUT DIODE CAPACITY PULSE. (BETWEEN .5 & 1 M).

‡ TRIM TO MAKE 20v = 100 μA NORMAL AND 2v = 100 μA ON NARROW CHANNEL.

FIGURE 11:

PULSE AMPLITUDE ANALYSER – DISCRIMINATORS

vii. Associated Equipment. The circuits for the side-channel pulse amplitude analyzers, gate-pulse generator, and biased-amplifier are given in Figs. 8,9,10,11. Since these are standard circuits, a detailed description of their operation will not be given here.

3. Performance of the Time-Sorter.

With diphenylacetylene crystals used in the scintillation counters, and the circuit operated under the conditions described in the previous pages, the following performance data were obtained.

A. Resolution. A resolution curve of effective width $2\tau_o$ of 1.1×10^{-9} sec. was obtained using an As^{76} source of coincident gamma rays of energy 1.20 and 0.57 Mev., (Fig.12). The reason that the resolution time ($2\tau_o$) calculated from these curves is less than that obtained by Bell et al. (1952), is due to the fact that the delay corresponding to the width of one channel on the kicksorter ($2\mathcal{T} = 1.8 \times 10^{-10}$ sec.) is shorter than the equivalent quantity* in the circuit of Bell et al; namely, the *equalized pulse* length. ($2\mathcal{T} = 1.5 \times 10^{-9}$ sec). It is shown in Appendix A, that the effective width of the resolution curve is given by: $2\tau_o = \frac{2\mathcal{T}}{1 - e^{-\mathcal{T}/\bar{t}}}$, where $\bar{t}$ is the mean time delay for the appearance of the first photo-electron,

---

* See Appendix A.

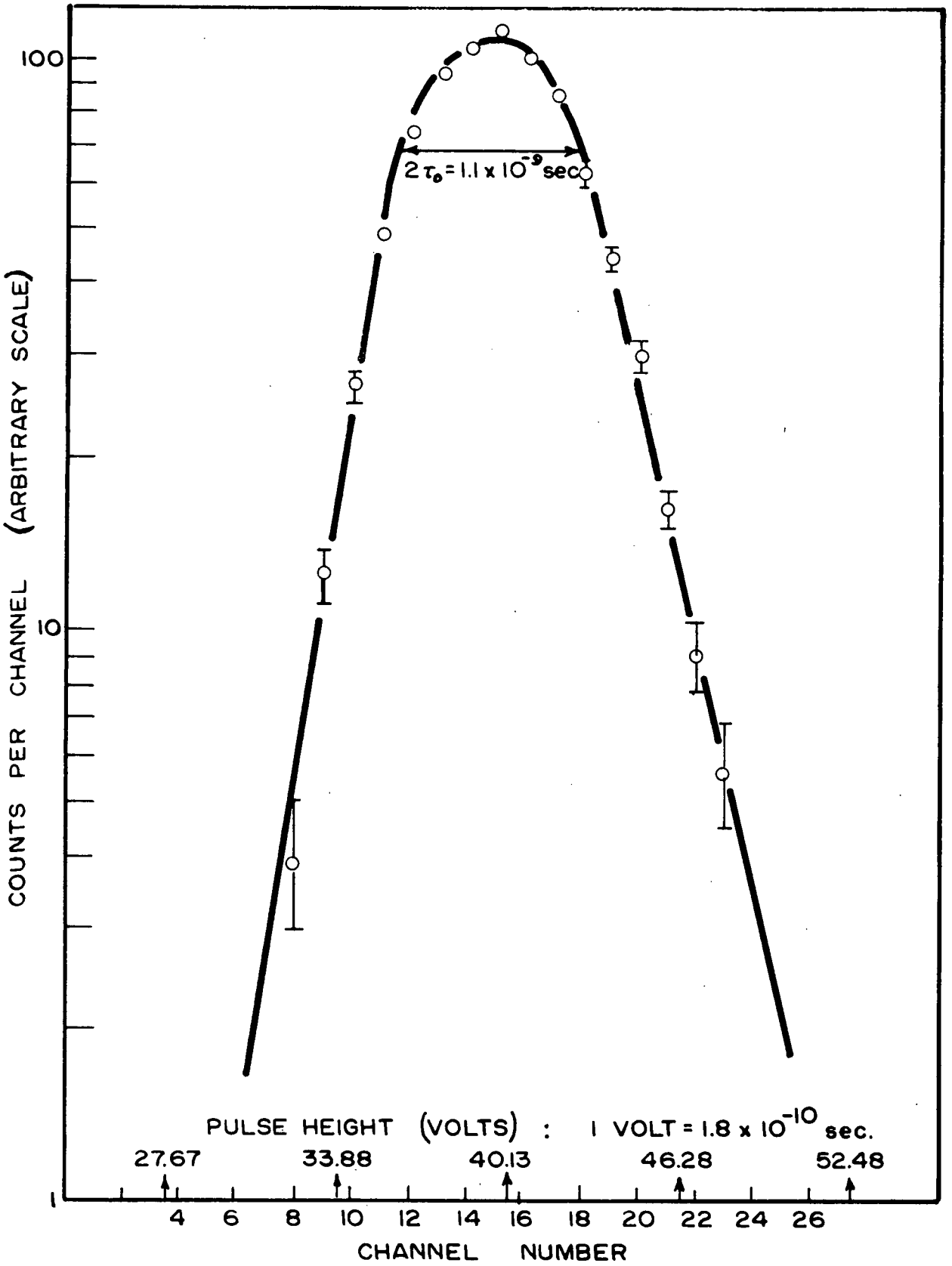

FIGURE 12: As^{76} COINCIDENCE RESOLUTION CURVE

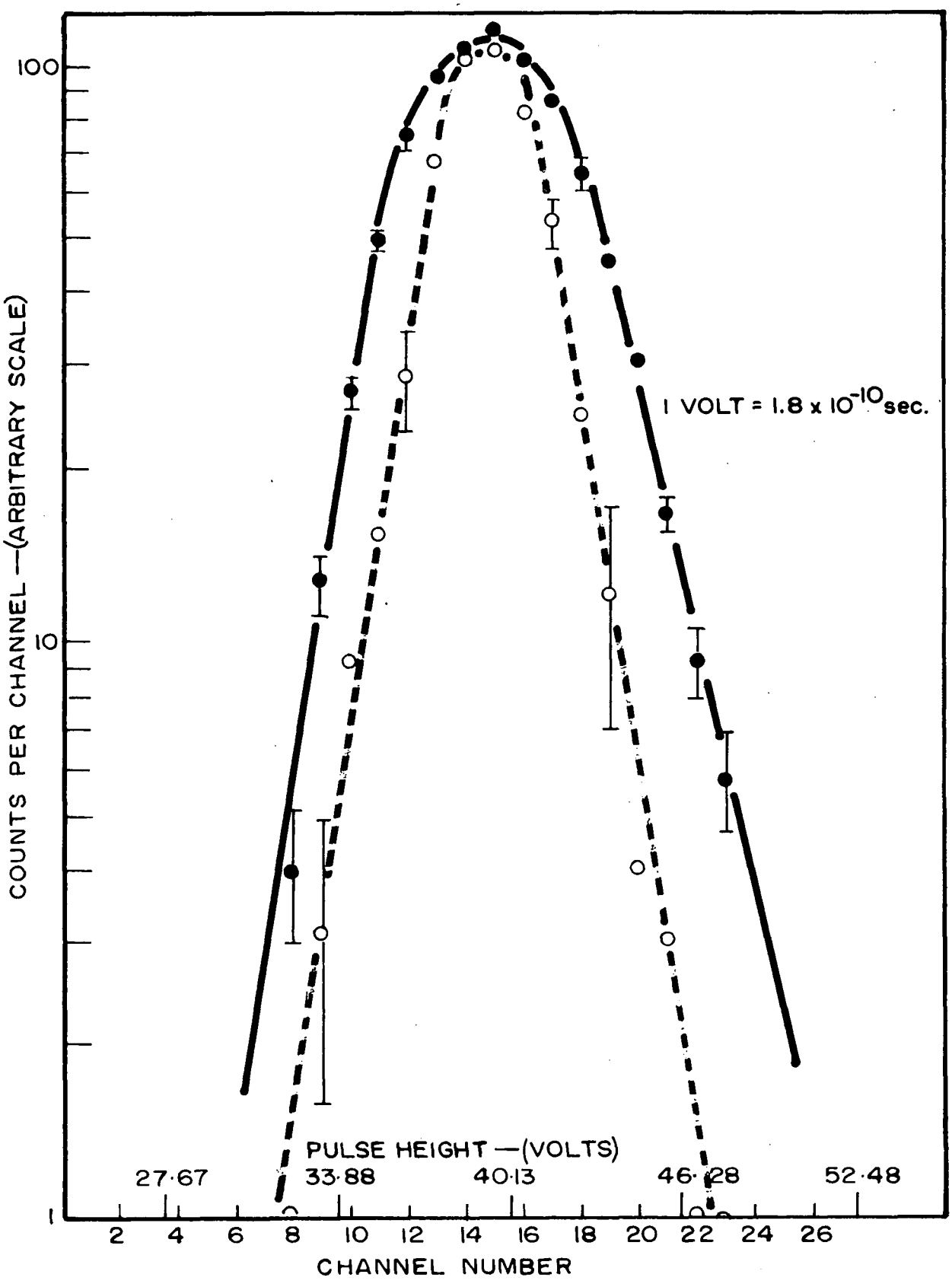

FIGURE 13: EFFECT OF SIDE CHANNEL DISCRIMINATOR SETTINGS ON THE RESOLUTION TIME

(Solid line corresponds to wider Side Channel window)

the electron transit-time spread of the photomultiplier being assumed negligible (Bell et al. 1952). In the circuit of Bell et al. (1952), where τ is much greater than $\bar{t}$, the effective width of the coincidence resolution curve approaches 2τ. However, as the time τ becomes small, the resolution time approaches the value $2\bar{t}$.

Figure 13 shows the dependence of the resolution time of the coincidence resolution curves on the side-channel pulse-amplitude analyzer settings, illustrating the effect described in section v, Chapter II, 2. The source used in this case was an As^{76} gamma source. For the As^{76} and Na^{22} resolution curves, one of the side-channel pulse-amplitude analyzers was set so that only pulses corresponding to the Compton electrons arising from the 500 Kev. gamma rays would be registered, while the other was set in a similar fashion for the Compton electron pulses of the 1.20 Mev. Gamma rays.

The slopes of the As^{76} curves (Fig. 12) indicates that the coincidence rate drops by a factor of two in 1.9×10^{-10} sec. (left) and 2.3×10^{-10} sec. (right), indicating that the inherent resolution of the apparatus (determined chiefly by the counters), is comparable with that obtained by other workers (Bell et al. 1952).

B. Stability. Figure 14 illustrates the stability obtained. The curve of Fig. 14a was obtained in four hours one afternoon, while that of 14b was the result of a ten hour

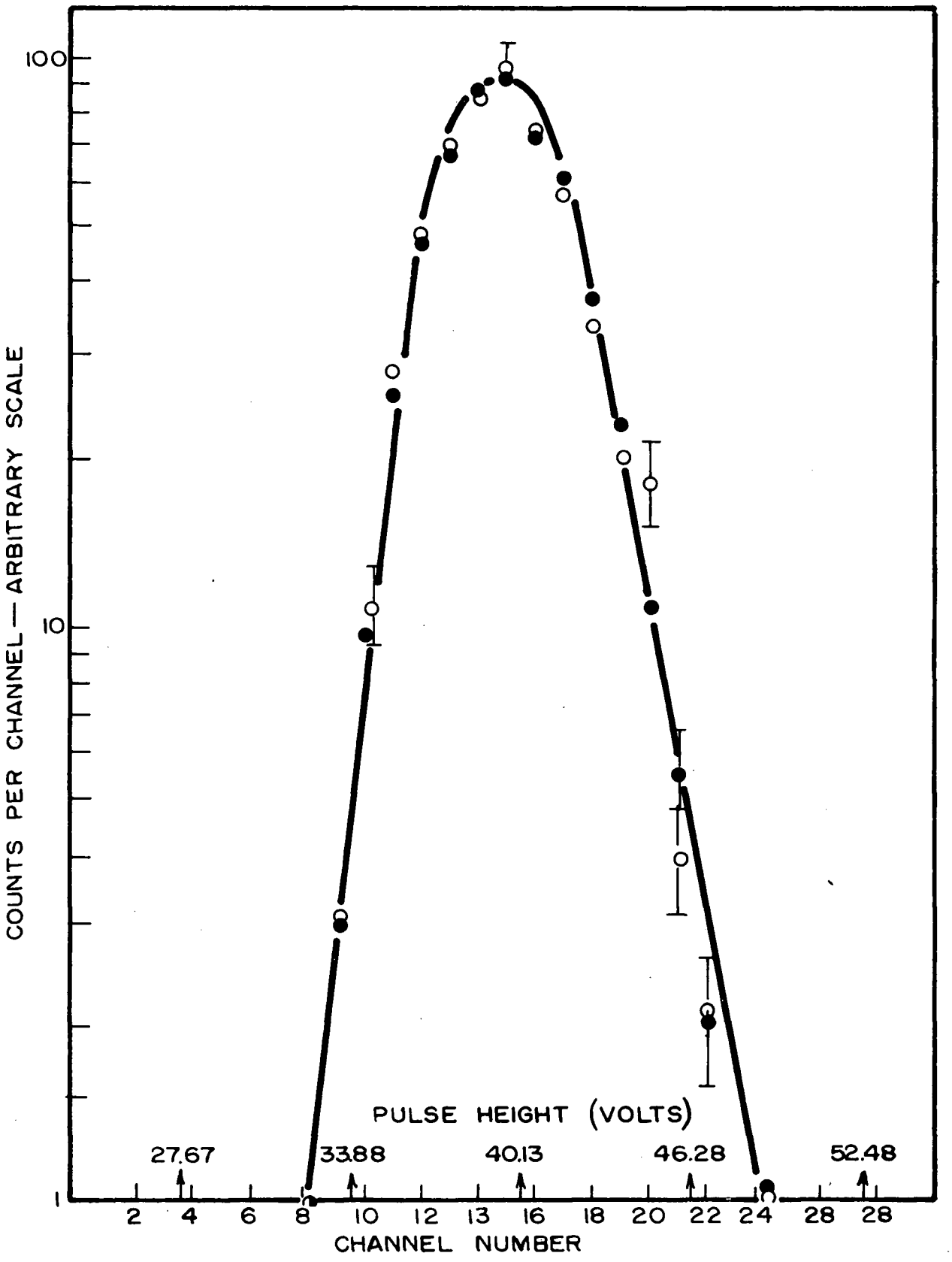

FIGURE 14: COINCIDENCE RESOLUTION CURVES ILLUSTRATING STABILITY OF TIME-SORTER

(a) Open Points (b) Solid Points

run over-night. It is evident that the stability of the device was quite satisfactory. Over a period of at least a day, the mean of a coincidence resolution curve could usually (80% of the time) be reproduced within a tenth of a kick-sorter channel width.

The stability of the apparatus would probably be improved by incorporating a d.c. current stabilizer in the limiters, to ensure long-term stability of the anode current.

Also, the insertion of a boot-strap or clamping circuit in the d.c. restoration portion of the limiter cathode circuit would enable the toleration of higher counting rates (Lewis and Wells 1954).

C. Linearity. One obvious disadvantage of this circuit as compared to the original Bell et al. (1952) circuit is the lack of a completely linear time calibration for the experimental curves. In order to keep the conducting resistance of the diode constant for the overlap pulses, the voltage drop across the diode must be kept constant. This can be accomplished if the diode output pulse is kept much smaller than the input overlap pulse (by employing a large integrating capacitor). An actual Miller integrator rather than the capacitor itself (as in the circuit of Neilson and James 1955) offers advantages in this respect. However, the ability to retain the very high frequency components necessary in these measurements sets a very severe restriction on the electronics employed. Also, the size of the integrating capacity is

limited by the requirement that the output pulses be kept well out of the noise region for good resolution. For these reasons the use of the ceramic capacitor was deemed advisable. Actually, with an integrating capacity of about 40 pf., one is able to operate the time sorter in a linear portion of the calibration curve by choosing a suitable degree of pulse overlap for the prompt point, as is shown in Fig. 21. This calibration curve can be obtained quite readily by observing the peak shifts of a prompt source as a function of either inserted delay or gamma-ray time of flight when using a source of coincident gamma rays.

4. Discussion of Circuit.

The circuit described in the previous pages, although essentially the same as the Bell et al. (1952) fast coincidence circuit as far as the actual components are concerned, has, with some circuit modifications of the coincidence detector, been operated in a fashion similar to that of the time-sorter of Neilson and James (1955). This type of operation lends itself to an improvement in the resolution time obtainable without an undue loss in counting rate, and enables the investigator to secure his data with greater speed, since the whole coincidence resolution curve is recorded simultaneously.

CHAPTER III

USE OF THE FAST TIME-SORTER TO MEASURE LIFETIMES OF POSITRONS IN ALUMINIUM AND MICA

1. Discussion of Positron Decay in Metals

A. Summary of Previous Results. The mode of annihilation of positrons in various materials follows a fairly complex pattern. In gases, both two-photon and three-photon annihilations are observed (Deutsch 1951) and have been attributed to the annihilation of para- and ortho-positronium respectively. In many amorphous and liquid substances, the three-photon decay is relatively weak. The two-photon decay, however, is characterized by the presence of two lifetimes, one short, (of the order of 5×10^{-10} sec.) and one long (about 3×10^{-9} sec.), with relative intensities of about 2:1, which remains fairly constant from substance to substance (Bell and Graham 1953). The same authors attribute the longer lifetime to conversion of the triplet positronium to the singlet state by collisions with atoms of the sample material. The annihilation probability of the "long" lifetime is then determined by the conversion rate. Dixon and Trainor (1955), on the other hand, believe the long-lived component to be due to direct annihilation from the second excited state of singlet positronium.

In metals, only the short-lived component of the positron lifetime is observed. Millett (1951) was one of the first to attempt to measure the lifetime of Na^{22} positrons in metals, viz. gold and lead. His results of 9×10^{-10} sec. were obtained by measuring the slope of his delayed coincidence resolution curve. Since his results do not agree with subsequent measurements, one can probably assume that the above figure was the inherent uncertainty introduced by his apparatus, and that a truly "prompt" resolution curve would possess essentially the slope quoted. De Benedetti and Richings (1952) then published a list of differences in positron half-lives between aluminium and other metallic and amorphous substances. Their results indicated that the lifetime of positrons in metals was constant within 0.5×10^{-10} sec. Next, Bell and Graham (1953) measured the absolute lifetime of positrons in various materials, and found that in all metals the lifetime was $(1.5 \pm 0.5) \times 10^{-10}$ sec. with a tendency for slightly shorter mean lives in metals of larger atomic number. Then Minton (1954) measured the absolute lifetime of positrons in aluminium and lead, obtaining the results, 2.9×10^{-10} and 3.5×10^{-10} seconds, respectively. Since Bell and Graham's work was more thorough than Minton's, their value of 1.5×10^{-10} sec. is the accepted mean lifetime of positrons in metals. The theoretical interpretation of this result, however, has not been altogether satisfactory.

i. Theory of Annihilation by Collision. Since no evidence of a long-lived component in the lifetime measurements was observed, the first approach at predicting the mean lifetime of positrons in metals was made by assuming that positronium is not formed, but that slow positrons annihilate during collision with free electrons with Dirac's cross-section for annihilation; $\sigma = \pi r_o^2 \, c/v$ (Heitler, 1954), where r_o is the classical electron radius, and v is the velocity of the positron relative to the electron. The total lifetime for annihilation of positrons would thus be the sum of the lifetime of the thermal positrons and the mean time required for the positrons to slow down. This latter time was first calculated by De Benedetti et al (1950) to be 3×10^{-10} sec. for metallic gold. A more detailed consideration of the collision phenomena involving slow positrons and conduction electrons by Garwin (1953) and Lee-Whiting (1955) led to a revision of the slowing-down time of positrons in metals to about 3×10^{-12} sec. Therefore, as far as the total lifetime of positrons in metals is concerned, the slowing-down time can be ignored.

Ore and Powell (1949) showed that the probability for annihilation of a positron with an electron when the spins are parallel is 1/1120 times the probability for annihilation when the spins are antiparallel, since such an annihilation must take place with the emission of three photons, a much less probable process than the emission of two photons.

Rich (1951) and De Benedetti (1954) have both observed a three-photon disintegration rate in aluminium which agrees with this value -- further evidence in support of the type of annihilation process assumed.

The probability of annihilation will be given by: (Bell and Graham 1953):

$$\lambda = \sigma N v$$

where σ is the Dirac cross-section, and N is the electron density. Thus $\lambda = \pi r_0^2 c N$ or τ, the mean life of the positron is:

$$\tau = \frac{1}{\pi r_0^2 c N} = 2.2 \times 10^{-10} \frac{A}{\rho N_e} \text{ sec.}$$

A being the atomic weight of the material of density ρ.
N_e is the effective number of electrons per atom of the metal.

The results of Green and Stewart (1955), and also Lang et al. (1955), indicate that positrons rarely annihilate with the electrons of atomic cores, but that they annihilate chiefly with the electrons of the Fermi Gas having the same density as that of the free, conduction electrons in the metal. Thus, N_e is given by the valence of the atom.

Applying these results to the cross-section formula, we find that the quantity $\frac{A}{\rho N_e}$ varies widely for different metals, being, for example, 2.44 for Beryllium and 23.7 for Sodium. This simple model of the annihilation process is therefore unable to account for either the shortness of the mean life in metals, or its constancy from metal to metal.

It has been suggested that Coulomb attraction may cause an increased electron density near the positron and hence a shorter lifetime (De Benedetti et al. 1950, footnote 18). It is doubtful, however, whether this factor could decrease the sodium lifetime, say, by a factor of at least ten. This statement is supported by the calculations of Ferrell (1955), who only predicts a decrease by a factor of two for the annihilation lifetime of positrons in sodium due to Coulomb enhancement.

Another method for attempting to correct this model would be to assume that the Dirac cross-section for annihilation is not inversely proportional to the first power of the relative velocity but to a higher power. However, the angular correlation results of Green and Stewart (1955) indicate that the $1/v$ dependence fits the experimental results most satisfactorily. If, though, a $1/v^2$ dependence is assumed, then the annihilation probability is proportional to $1/v$. In a Fermi electron gas, in which $n(p)dp$ is proportional to p^2dp, where $n(p)dp$ is the number of electrons per cc. with momenta between p and $p + dp$, we then find that the total annihilation probability, $\lambda_T = \int_0^{p_F} \lambda(p)\, n(p)\, dp \propto \int_0^{p_F} \frac{1}{p}\, p^2\, dp = \frac{1}{2} p_F^2$, and, since $D \propto p_F^3$ then λ_T, rather than being linearly proportional to D (the electron density), as before, is now proportional to $D^{2/3}$. Since a range in lifetimes from about 3×10^{-10} sec. for

beryllium to 22 x 10^{-10} sec. for sodium would still result with this hypothesis, a velocity dependence of $1/v^n$, with n greater than 2 would be required to decrease the lifetime variation from metal to metal. However, the angular correlation results of Green and Stewart (1955) requires $0 \leqslant n \leqslant 2$. Thus another interpretation of the phenomenon of positron annihilation is required.

ii. Theory of Formation of Positronium. The second approach at predicting the mean lifetime of positrons in metals was made by Bell and Graham (1953), who assumed that when positrons are slowed down to thermal energies, they have a high probability of forming the bound state, positronium, which then decays with its characteristic lifetime; the lifetimes of singlet and triplet positronium being 1.25 x 10^{-10} sec. and 1.4 x 10^{-7} sec. respectively. Dixon and Trainor (1955) state "that if positronium has a stable binding in solid media, then its formation is a highly nonequilibrium process. Once the positronium atom is formed it has a high probability of persisting until annihilation takes place, since the ionization energy required to free the pair is not readily available."

Since the momentum of the centre-of-mass of the annihilating pair determines the deviation from co-linearity of the annihilation gamma rays, "the positronium model" is consistent with the results of Green and Stewart (1955) if

the positron is assumed to be essentially at rest at the time of positronium formation. One might expect the positronium atom to retain its kinetic energy during collisions with other atoms of the metal because of its extremely low mass, although this seems unlikely because of the large number of collisions.

Since Bell and Graham's measurements (1953) of the lifetime of positrons in metals indicated a constant value of about 1.5×10^{-10} sec., the above interpretation seemed in agreement with their results, if one assumed that the slowing-down time of the positrons and the positronium formation time were negligible, and that only the singlet positronium was formed. However, it is difficult to conceive of such a process by a random collision of positrons with the electrons comprising a Fermi Gas. For this reason, it was suggested (Garwin 1953) that a rapid conversion process takes place between para- and ortho-positronium by electron exchange. In such a case, the probability that a positronium atom annihilate while in the triplet state is very small, equal, as a matter of fact, to the probability of a thermal positron annihilating with an electron when their spins are aligned in the same direction. This is stated as being 1/370 times as frequent as the two-photon annihilation rate (Ore and Powell 1949), a prediction in agreement with the experimentally determined three-photon annihilation rate in aluminium.

Doubt was cast on the validity of the above inter-

pretation of the data, however, when Garwin (1953) also remarked that a fast conversion process would lead to a lengthening of the short lifetime component by a factor of four, since the positronium atom would exist in the ortho-state 3/4 of the time and in the para-state only 1/4. Thus, assuming as correct the theoretical estimate of 1.25×10^{-10} seconds for the lifetime of para-positronium, a positron lifetime of 5×10^{-10} seconds would be expected, rather than the 1.5×10^{-10} sec. observed. Since this discrepancy has not been satisfactorily explained to date, it was deemed worthwhile to attempt to measure the absolute lifetime of positrons in a metal to check the results of Bell and Graham.

B. The Difficulties Inherent in Absolute Lifetime Measurements, and Their Solutions. In nearly all measurements of lifetimes by the delayed coincidence method, in which the lifetime measured is short compared to the resolution time of the instrument, a "prompt" resolution curve is needed to complete the analysis. One of the major difficulties associated with measuring short lifetimes is that of obtaining a suitable prompt source; the reason being that the "time of occurrence" of the counter pulse is a function of the energy dissipated in the phosphor (Post and Schiff 1950). It is therefore desirable to obtain as the prompt source, a source of gamma rays of the same energy as those being measured.

Failing this, side-channel selection could be employed to insure the equality of the amplitudes of both the prompt and delayed pulses.

1. Bell and Graham's Solution. Another method of circumventing this problem was that adopted by Bell and Graham (1953) in which the positron itself was used to produce both the prompt and delay pulses without the necessity of employing the 1.28 Mev. gamma ray as a zero time indicator. In one end of a beta-ray spectrometer they inserted a fast scintillation counter with a Na^{22} positron source imbedded in the crystal.. The pulse produced as the positron left this crystal provided the zero of time for the coincidence circuit. The positrons were selected in energy and trajectory by the spectrometer before striking either the crystal of the second counter to produce the prompt curve, or an absorber situated immediately in front of the second counter for the delayed curve. In the latter case the second counter observed the annihilation gamma rays rather than the positrons themselves.

This procedure possesses a number of advantages over simpler methods. It gives the value of the mean life absolutely, and not merely by comparison with that of another sample. The method does not depend on the nuclear properties of the source; and it is nearly free of chance coincidences, since nearly every true count in the sample counter corresponds to a coincidence event.

Some disadvantages are also associated with this method, however. The prompt curve consists of coincidences between pulses of constant amplitude in both counters due to the energy selection of the spectrometer. The delayed curve, however, consists of coincidences between pulses of constant amplitude for the "zero time" counter, and a spectrum of pulses from the second counter, (viz., the Compton spectrum of the 500 Kev. annihilation gammas). The symmetry of the arrangement is altered somewhat, since, in one case, the second counter views the primary positrons, and in the second, the annihiliation gamma rays of these positrons. Also, the positrons striking the second crystal for the prompt curve dissipate all their energy in a very short distance, causing the formation of the scintillations essentially at the front face of the one $cm.^3$ crystal. In the case of the delayed curve, the 510 Kev. gamma rays penetrate, on the average, some distance into the crystal before producing the scintillations. The exact effect of these phenomena on the measured lifetime is difficult to ascertain, and are not present in the other two methods of measuring the lifetimes.

ii. Minton's Method. Minton (1954) measured the lifetime of positrons in aluminium and lead, by using the 1.28 Mev. gamma ray of Na^{22} to determine the zero of time, and obtained the prompt curve by using the cascade gamma rays of Co^{60}. Coincidences between pulses originating from appropriate

parts of the gamma-ray Compton spectra were obtained by employing side-channel pulse amplitude selection. His results of 2.9×10^{-10} sec. for Al, and 3.5×10^{-10} sec. for Pb are in disagreement with the absolute measurements of Bell and Graham, although their difference of about 0.5×10^{-10} sec., is within the error of previous measurements. Due to the difficulty, however, in restricting the side-channel widths sufficiently to insure good equality of pulse amplitudes between the Na^{22} and Co^{60} sources, and still maintain an adequate counting rate, the desirability of using an "artificial" Na^{22} source for the prompt curve is obvious.

iii. The Artificial Na^{22} Method. By an "artificial" Na^{22} source is meant a source which emits two prompt gamma rays, one of energy near 1.28 Mev., and the other near 510 Kev. With such a source, similar spectra are produced by the counters for both prompt and delayed curves. Thus the differential pulse height selectors in the side channels need only define the pulse size sufficiently to prevent the resolution curve from being too broad.

2. The Measurement of the Absolute Lifetime of Positrons in Aluminium.

A. Use of As^{76} as the "Prompt" Source. A search of the literature on Nuclear Data and decay schemes indicated that As^{76} might be a suitable prompt source. The following relevant data were obtained: (Hubert 1953).

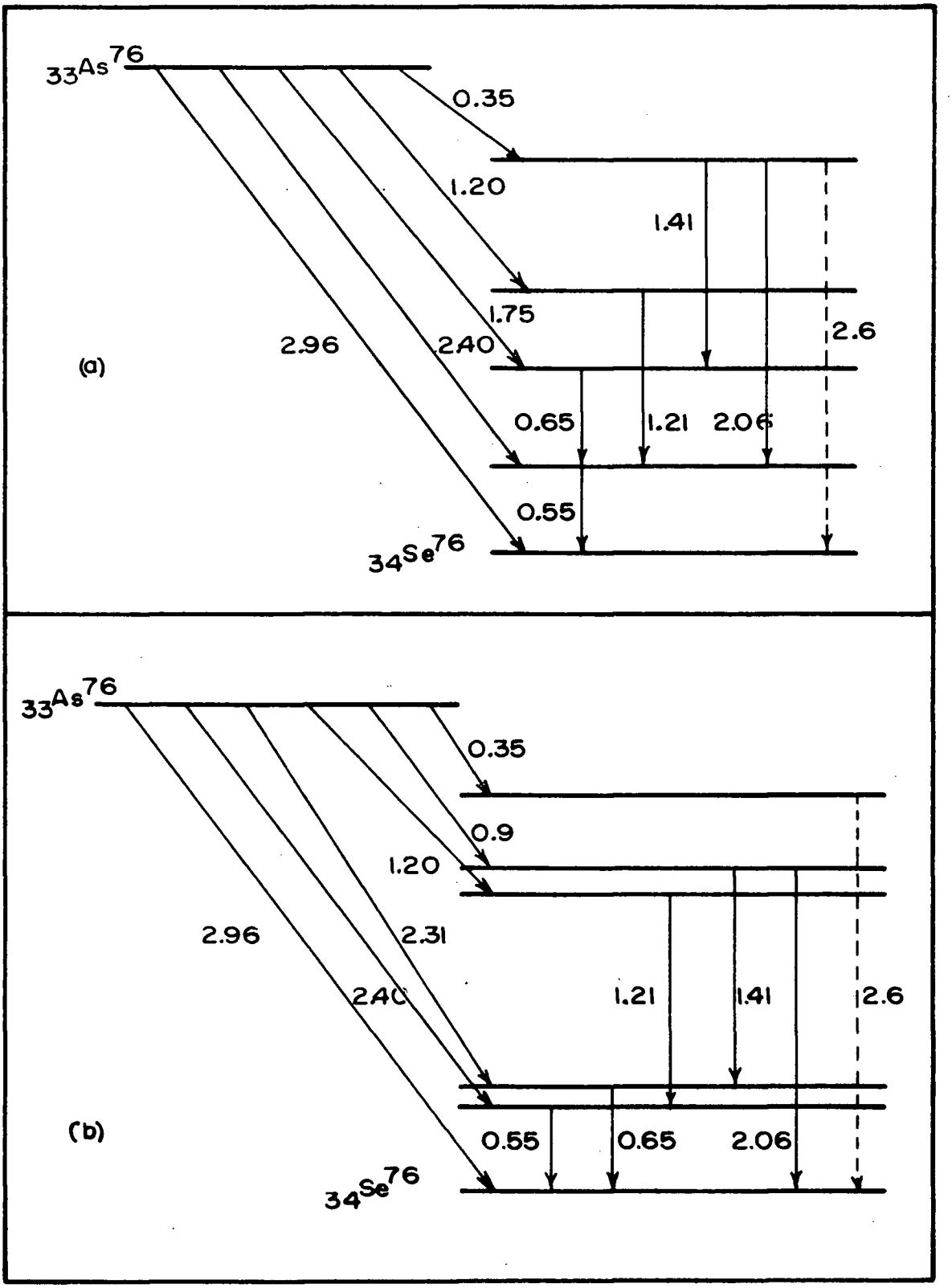

FIGURE 15: DECAY SCHEME OF As^{76} (a) Favoured Scheme

(b) Alternative Scheme

GAMMA NO.	ENERGY IN MEV.		RELATIVE INTENSITY	
	COMPTON	PHOTOELECTRONS	COMPTON	PHOTOELECTRONS
1	0.550	0.553 ± 0.002	1	1
2	——	0.648 ± 0.002	0.07 ± 0.04	0.095 ± 0.01
3	1.17	1.210 ± 0.005	0.21 ± .04	0.25 ± 0.02
4	1.4	1.410 ± 0.006	0.014 ± 0.005	0.016 ± 0.004
5	2	2.06 ± 0.01	0.04 ± 0.01	0.055 ± 0.01

TABLE 1: As^{76} GAMMA RAYS (Energy and Relative Intensity)

i. The half-life of As^{76} is 26.7 hours, of suitable duration for many runs with the apparatus.

ii. It possesses cascade gamma ray energies of 1.21 Mev., and 555 Kev. (see decay schemes, Fig. 15; scheme 1 being the favoured one).

iii. A necessary requirement for the use of As^{76} as a prompt source, is that the first excited state of Se^{76} have a very short lifetime. It appears that a reasonable estimate of the lifetime of the 560 Kev. state of Se^{76} is a few times 10^{-11} sec. (Stewart 1955).

iv. The energies and relative intensities of the gamma rays are given in Table 1, indicating that the 550 Kev. gamma ray and the 1.21 Mev. gamma ray are certainly the most intense, the other gamma rays being relatively weak except for the 650 Kev. gamma ray, which is 0.4 times the strength of the 1.2 Mev. gamma. However, since only the 550 Kev. gamma ray is in coincidence with the 1.21 Mev. gamma ray, the presence of the 650 Kev. gamma should have no effect on the resultant coincidence resolution curve except to increase the chance background.

Possible competing sources of coincidences are possible from the 1.41 Mev, 0.65 Mev. and 2.06, 0.55 Mev. pairs of cascading gammas. One would expect from intensity considerations, however, less than 5% of the total number of coincidences to be due to the former, and a correspondingly small

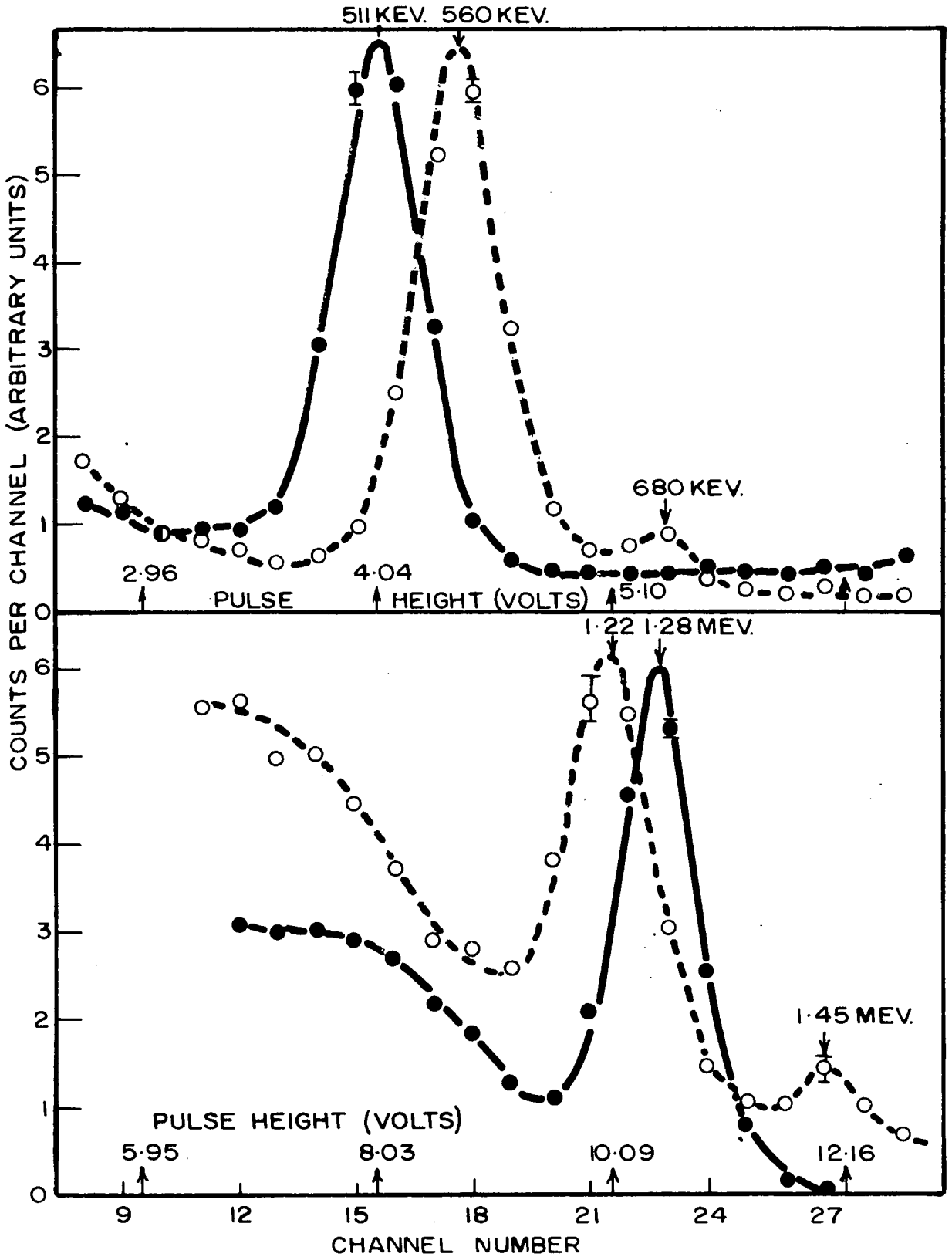

FIGURE 16: GAMMA-RAY SPECTRA OF As^{76} (DOTTED CURVE) AND Na^{22} (SOLID CURVE) USING NaI CRYSTALS

contribution from the latter, since the side-channel window, set at the Compton edge of the 1.2 Mev. gammas, would be viewing a relatively low intensity portion of the Compton spectrum arising from the 2.06 Mev. gamma ray. If decay scheme two (Fig. 15) were found to be the correct one, then only the first-mentioned competing source of coincidences would be present.

v. The NaI spectra of As^{76} and Na^{22} are given in Fig. 16 to indicate the basic similarity of the two sources. The relative intensities of the two gamma rays being the chief difference between the two curves.

vi. Since the NRX reactor at Chalk River was inoperative at the time the experiment was performed, the As^{76} source was obtained by means of neutron bombardment of As^{75}. The neutrons were produced by means of a prolific (d,n) reaction using the deuterons accelerated by the U.B.C. Van De Graaff generator. For this purpose, it is indeed fortuitous that natural arsenic is composed totally of the As^{75} isotope.

B. Preparation of the Sources.

i. Na^{22} in Aluminium. The Na^{22} in aluminium source consisted of an aluminium rod of dimensions 6 in. x 1/4 in. One end of which was drilled out to a diameter of 1/8 in. and contained a deposit of Na^{22} Cl. Thus, no intermediate absorber, such as mica backing, etc. was employed. It was assumed that the fraction of positrons stopping in the NaCl

was negligible, due to the high specific activity of the salt. The source strength was about 0.01 mc.

ii. As^{76} in Aluminium. To obtain a source as nearly equivalent to that described in (i) above, $As_2^{75}O_3$, prior to bombardment, was placed in an aluminium capsule, also. The capsule (size 2½ in. x 3/8 in.) was of necessity slightly larger than the Na^{22} source, however, in order to obtain a sufficiently strong source. Prior to bombardment, the source was composed of chemically pure, 99.95% As_2O_3. The thermal neutron cross-section for As^{75} is quoted as four barns[1], whereas the cross-section for oxygen is only 0.2 mb., and is less than six barns for all the impurities quoted in the analysis of the As_2O_3 sample. Thus it was felt that no appreciable impurity activities would be produced.

Another reason for using an aluminium container lay in the fact that aluminium possesses one of the smallest thermal neutron cross-sections of all metals, (0.2 barns). Since the half-life of Al^{28} is only 2.3 minutes, the residual activity at the time the experiment was begun (a few hours later), was thus of negligible intensity.

a. The Reaction Employed. For the production of neutrons, the reactions $H^2(d,n)He^3$, $Be^9(d,n)B^{10}$, and $Li^7(d,n)Be^8$

---

[1] Handbook of Chemistry and Physics, 35th edition. Published by: Chemical Rubber Publishing Co. 2310 Superior Ave. N.E. Cleveland, Ohio

were considered. These reactions are listed in terms of increasing neutron yield for deuteron bombarding energies greater than one Mev. The $Li^7(d,n)Be^8$ reaction, however, is extremely exoergic, with about 15 Mev. neutrons being emitted, (Ajzenberg 1955). The $Be^9(d,n)B^{10}$ reaction, on the other hand, has a high yield of slower neutrons (about 10^{10} neutrons per sec. per microamp. of d) with the peak occurring at about 3 Mev. (Segrè, 1953).

For this reason, and the ready availability of thick Be^9 targets, the beryllium reaction was chosen for the production of neutrons.

b. The Target Assembly. The target assembly consisted of a lump of beryllium of unknown purity fastened to a brass endplate which was provided with a brass tube for circulating cooling water. Paraffin wax sheets were then stacked in a criss-cross fashion around the target assembly to act as a moderator, the final dimensions of the paraffin box being about 55 cm. along each edge, with the length of the cube extended in the direction of the beam to a distance of about one meter. A vertical hole reaching to the target assembly was left in the paraffin stack to allow access to the As^{75} sample, which was suspended in the center of the pile near the target.

c. The Bombarding Conditions. The target assembly was bombarded for 4½ hours with a deuteron beam of about 19

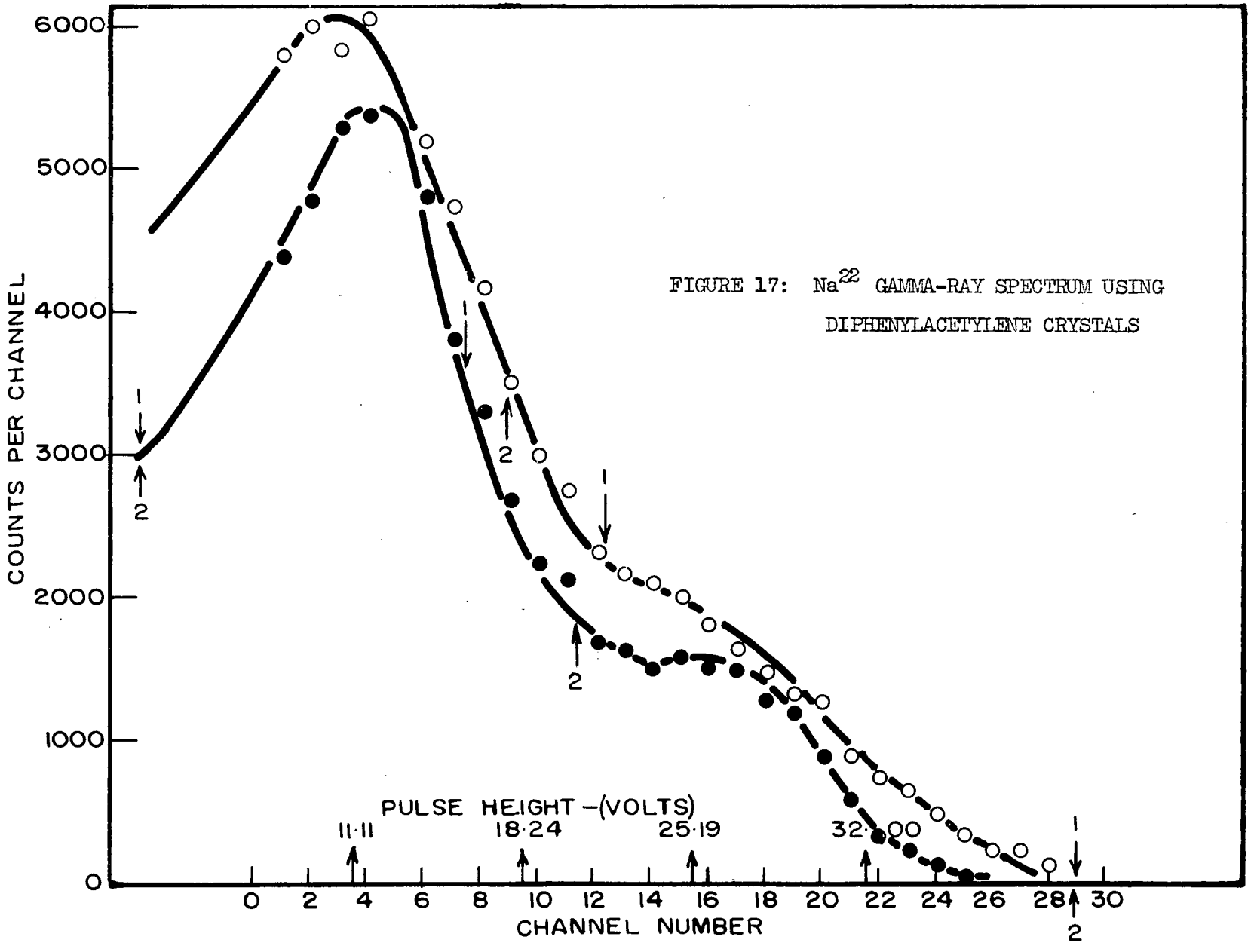

FIGURE 17: Na^{22} GAMMA-RAY SPECTRUM USING DIPHENYLACETYLENE CRYSTALS

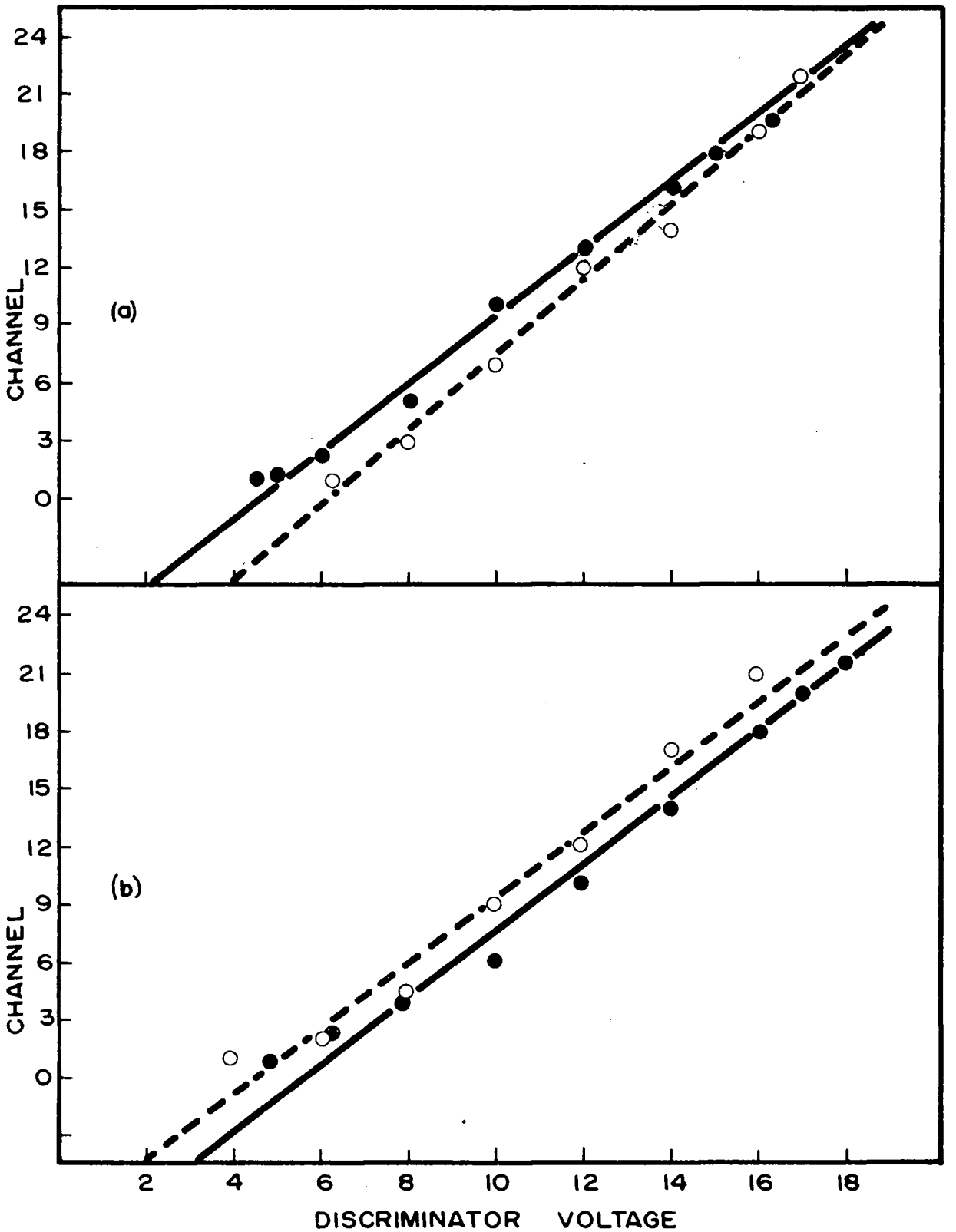

FIGURE 18: SIDE-CHANNEL ENERGY CALIBRATION CURVES

(a) Counter 1 (b) Counter 2

Dotted Curve: Upper Discriminator

Solid Curve: Lower Discriminator

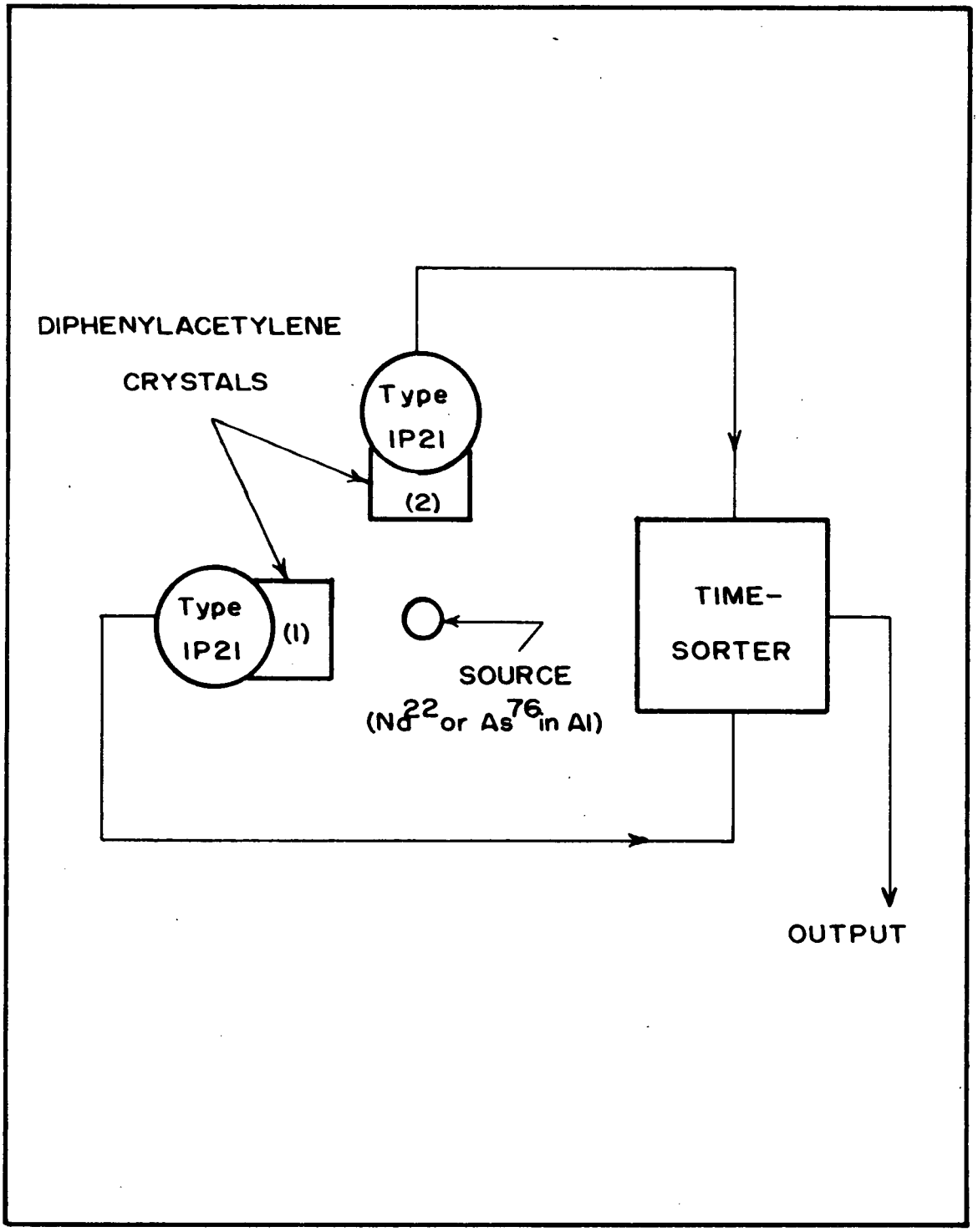

FIGURE 19: EXPERIMENTAL ARRANGEMENT

microamps. (average) at an energy of 1.6 Mev. The fraction of the beam hitting the Be^9 target was found to be quite large ($\sim$ 90%), judging from the darkened area of the target after bombardment. The final strength of the As^{76} source after the above exposure to slow neutrons was about 1/5 that of the Na^{22} or about 0.002 mc.

C. The Experiment.

i. The Experimental Procedure. After the Na^{22} spectra (Fig. 17) were obtained using the two diphenylacetylene crystals, the side-channel discriminator voltages were calibrated in terms of energy dissipated in the crystals. These calibration curves are given in Fig. 18. In the experimental arrangement of Fig. 19, the distance between the counters and the As^{76} source was usually about 3 mm., while distances of about two cm. were kept between the Na^{22} source and the counters, in order to keep the counting rates in each counter more nearly equal. The side channels were set at the bias points indicated by the arrows, (superscript one), on the spectra of Fig. 18 but were widened as illustrated by the arrows, (superscript two), after running about ten hours, in order to increase the coincidence counting rate, since the As^{76} source had decayed to nearly 1/2 the original intensity. The procedure while making these runs was to alternate between the As^{76} and the Na^{22} sources, so that an analysis of the results could be obtained, should slow gain shifts of the apparatus occur. An example

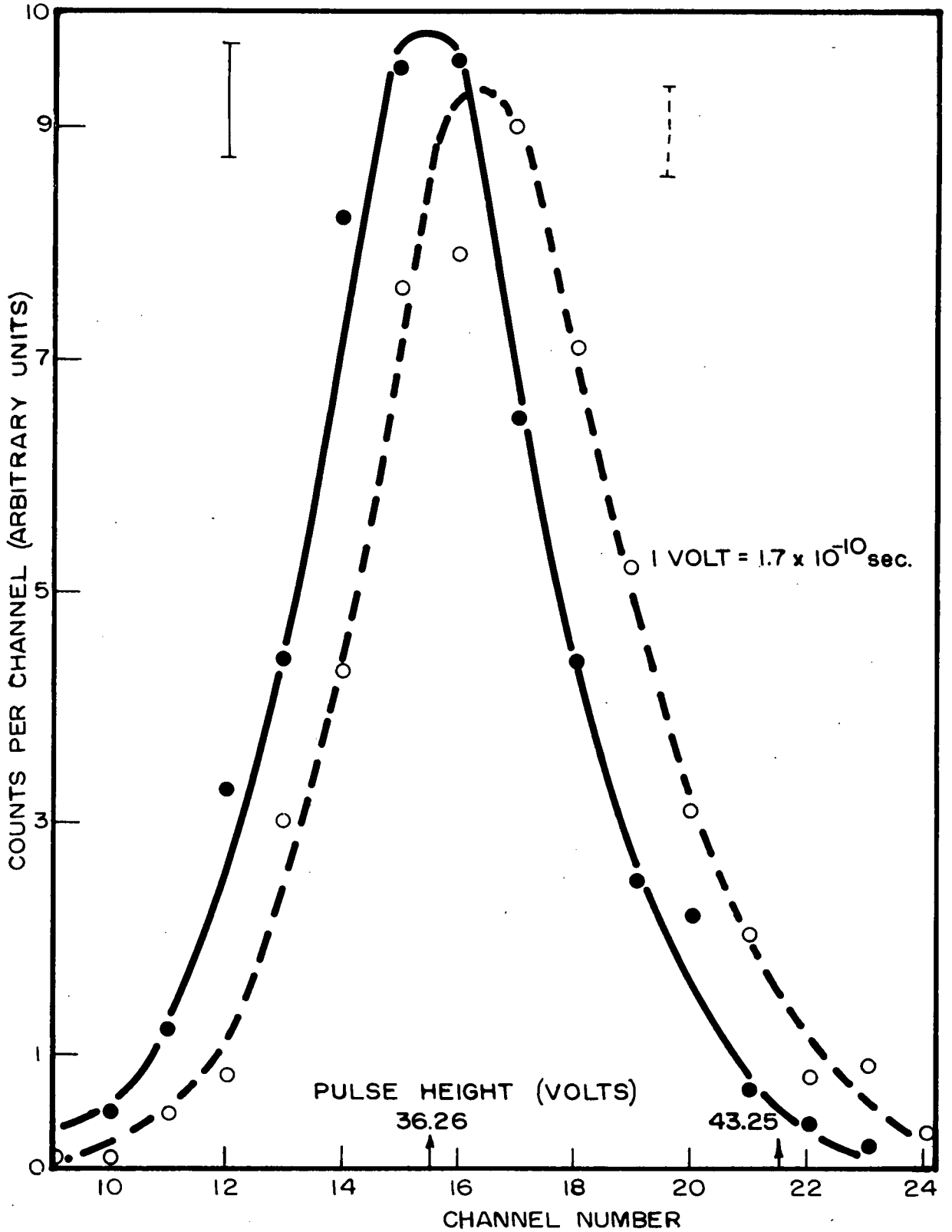

FIGURE 20: EXAMPLE OF COINCIDENCE RESOLUTION CURVES OBTAINED FOR POSITRONS ANNIHILATING IN Al (Dotted Curve) (Solid line is As^{76} "Prompt" Curve)

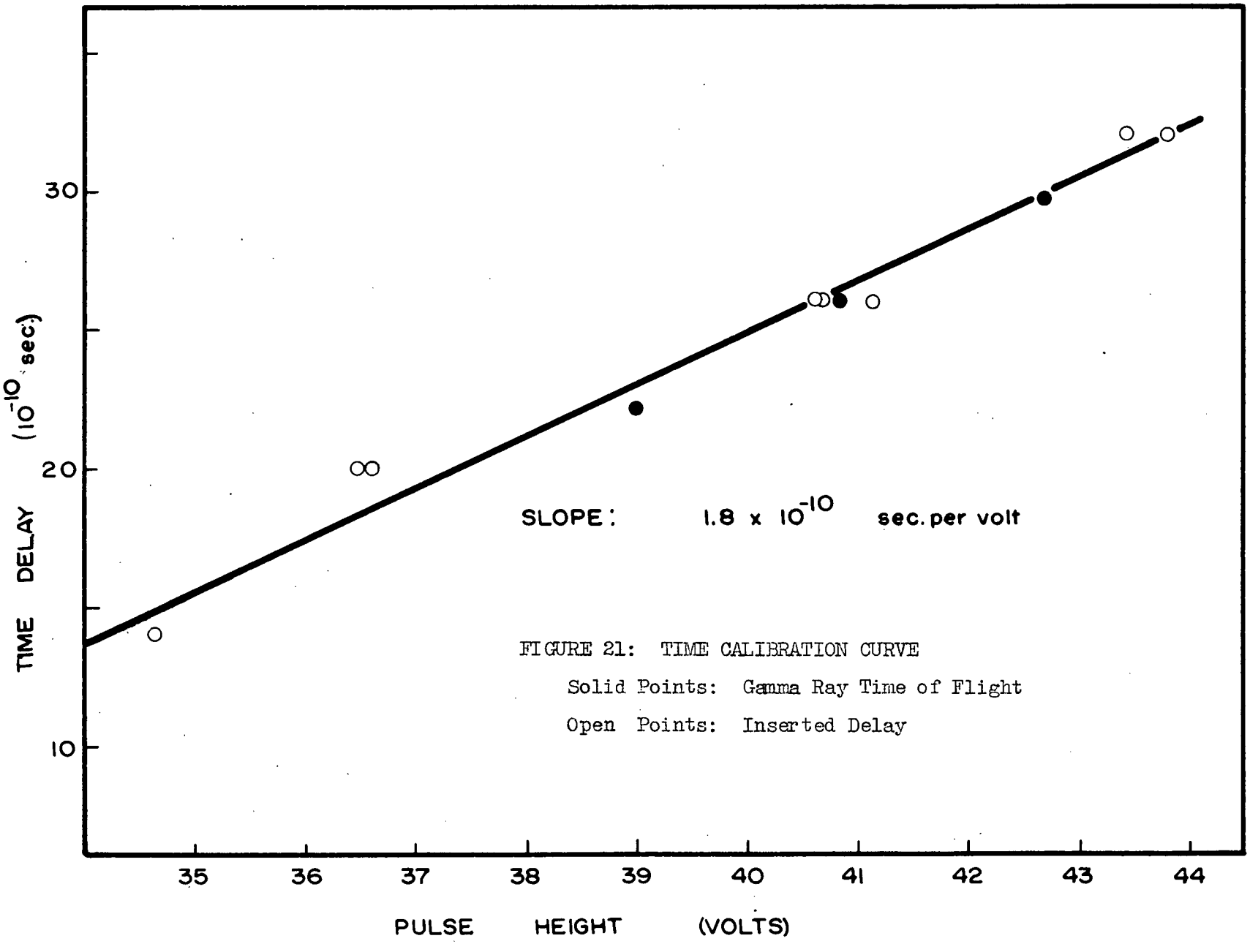

FIGURE 21: TIME CALIBRATION CURVE

Solid Points: Gamma Ray Time of Flight

Open Points: Inserted Delay

of the resulting curves are illustrated in Fig. 20. Analysis of the coincidence resolution curves was carried out by measuring the centroid shifts (see Appendix C). This method applies to the time-sorter resolution curves, as long as the curves are obtained while operating in a linear region of the instrument.

ii. The Time Calibrations. The time calibrations illustrated in Fig. 21 were also taken at this time and are based on voltage shifts of the peak due to both inserted time delay and gamma-ray time-of-flight.

iii. Pulse Height Dependence on Counting Rate. Since the counting rate with the As^{76} source in place was about twenty times slower than when using the Na^{22} source, it was necessary to determine whether the pulse height output from the apparatus was a function of counting rate. This was accomplished by obtaining coincidence curves using the Na^{22} source (1.28 Mev. and .511 Mev. coincidences). Different coincidence counting rates were obtained by varying the distance between the source and the two counters, (the gamma-ray path length being kept equal for both counters). The centroids of the coincidence resolution curves were then plotted against coincidence counting rate. The curve of Fig. 22 was the result of this test, indicating a positive dependence of pulse height on counting rate for the rates used.

The lifetime measurements were then obtained by

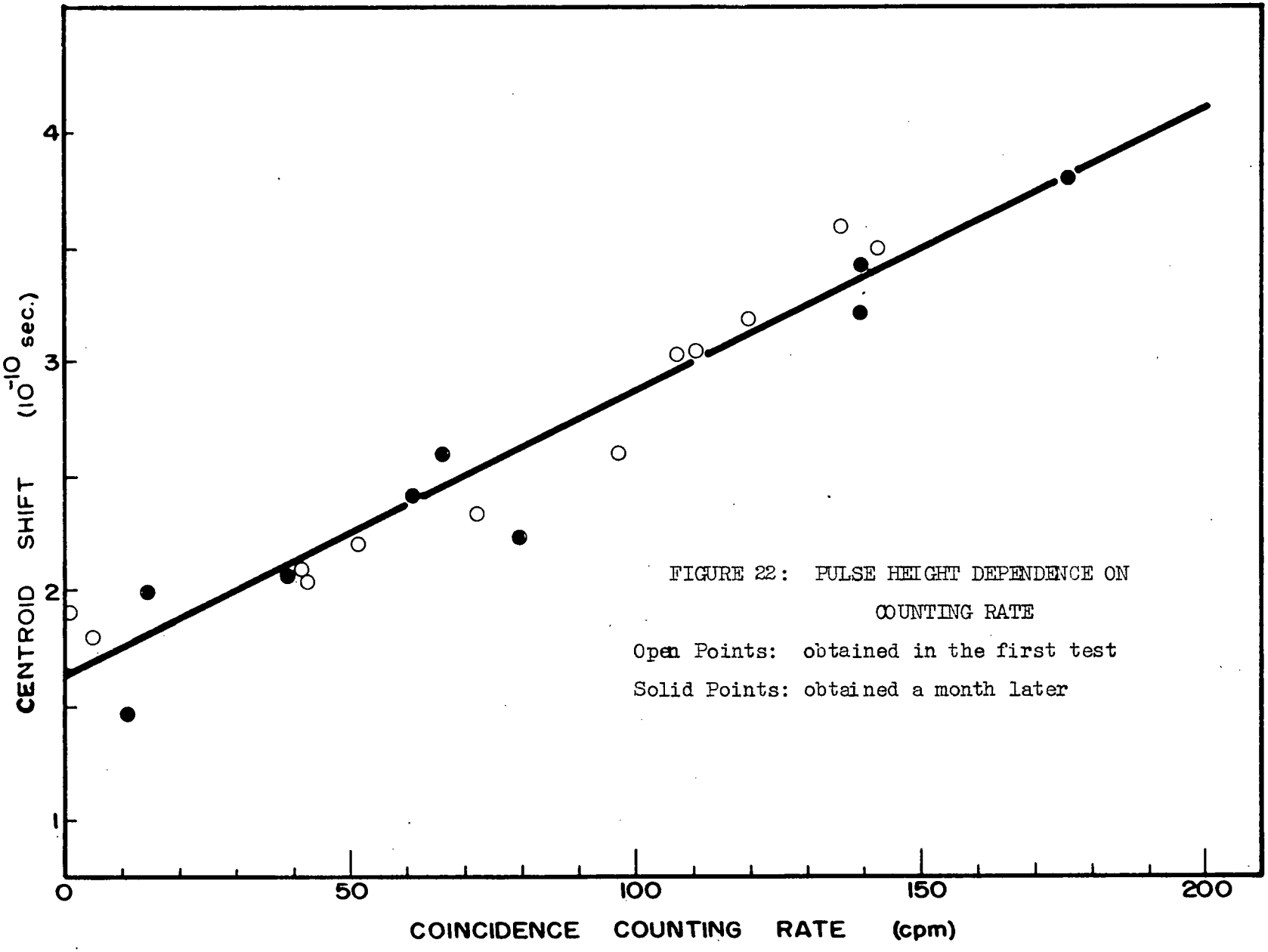

FIGURE 22: PULSE HEIGHT DEPENDENCE ON COUNTING RATE

Open Points: obtained in the first test

Solid Points: obtained a month later

correcting the centroids of the Na^{22} resolution curves for this dependence, normalizing all runs to the coincidence counting rate obtained when using the As^{76} source. Since the lifetime measurement obtained is such a critical function of this pulse height dependence on counting rate, the reproducibility of the pulse height calibration curve was tested by repeating the counting-rate dependent resolution curves a month later, under slightly different experimental conditions. The reproducibility was found to be very good, the latter curve being almost an exact replica of the previous one (with the slopes the same within 5%).

iv. Results. The average centroid shift (corrected for counting rate variations) of the positron-in-aluminium resolution curves as compared to their respective "prompt" curves, indicates a mean life τ, for positrons in aluminium of 1.6×10^{-10} sec. To allow for the errors in the various calibration curves, a total experimental error of 0.4×10^{-10} sec. is given for these results. Although the resolution is not sufficient to determine whether the decay is exponential, the results are consistent with this assumption (Newton 1950).

3. The Measurement of Positron Lifetime in Mica. In order to check that the apparatus was not introducing systematic errors in the above measurements, it was considered advisable to measure, under the same experimental conditions, the lifetime in another absorber, to determine whether the difference

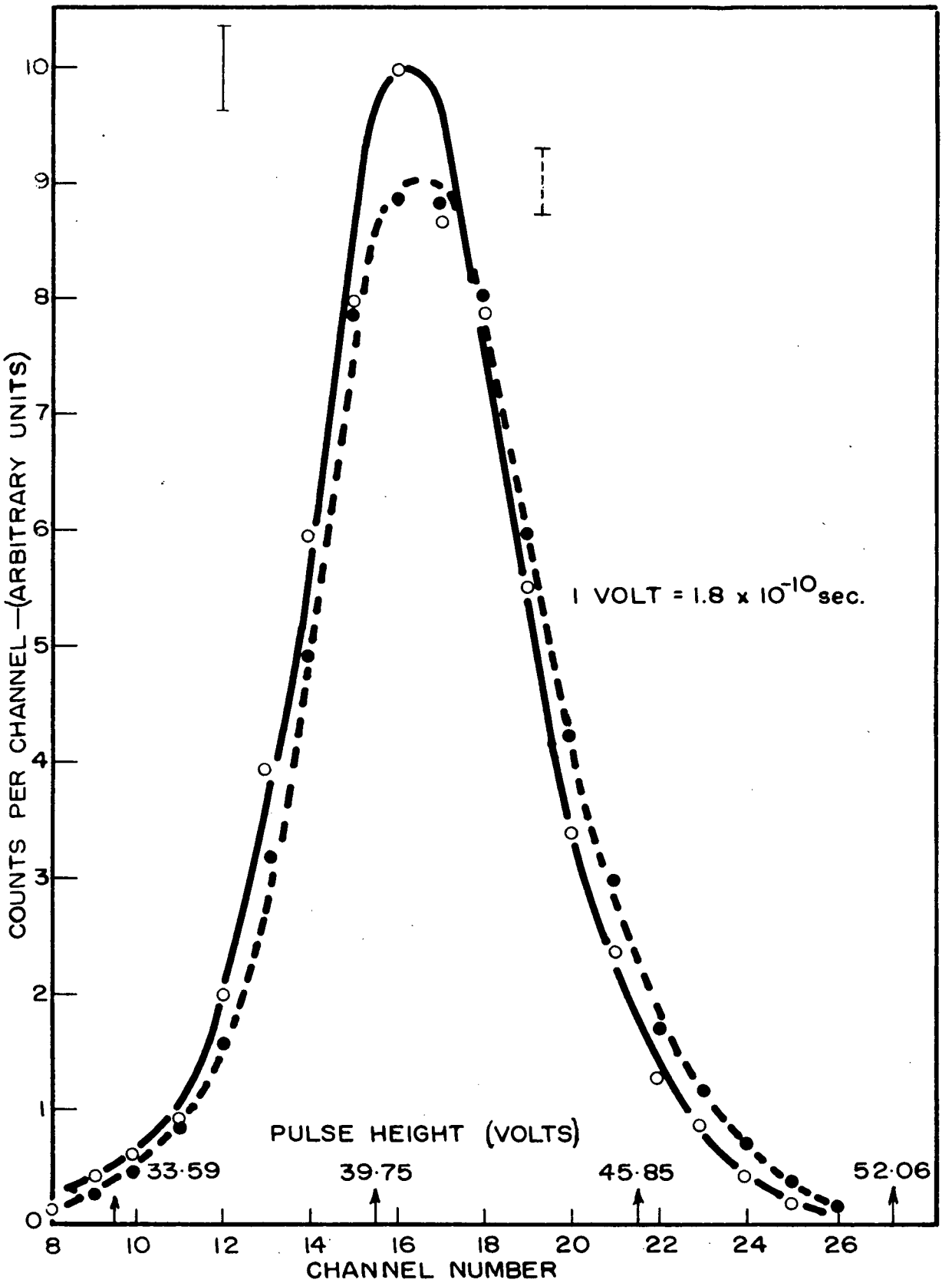

FIGURE 23: COINCIDENCE RESOLUTION CURVES

Comparison Curves for Positron Annihilation in Al and Mica

in lifetime between this new absorber and aluminium were consistent with the accepted results.

A. Method. Since the arsenic source had decayed to a prohibitively low strength by this time, it was decided to measure the positron lifetime in mica by the comparative method of De Benedetti and Richings (1952).

B. Procedure. Resolution curves for the positron lifetime in aluminium and mica were obtained, alternating from one absorber to the other. The Na^{22}-in-aluminium source was that used in the previous experiment. The mica-absorber source consisted of a small deposit of activated NaCl (about .05 mc) on the center of a .003 in. mica strip (about 0.7 cm x 1.5 cm.). This strip was then covered on both sides with sufficient mica to completely stop the most energetic positrons. Thus, neither source required corrections for positron absorption by the source material. The experimental arrangement was the same as before, with the "mica" source substituted for the As^{76}.

C. Results. The two resolution curves are illustrated in Fig. 23. When the centroids of these curves were calculated, a shift of $(0.7 \pm .4) \times 10^{-10}$ sec. was obtained, in agreement with the measurements of Bell and Graham (1953).

4. Discussion and Conclusions. It is interesting to note that the results of this experiment are in agreement with the

measurements of Bell and Graham (1953) of the half-life of positrons in Aluminium (1.5×10^{-10} sec.), rather than those of Minton (1954) (2.9×10^{-10} sec.). As described before, all three experiments involved different methods of obtaining the prompt resolution curve.

i. Bell and Graham's method: that of using the positrons themselves, after appropriate energy selection, to obtain the prompt curve; the zero of time being determined by passing the positrons initially through a thin stilbene crystal, and the associated "prompt" pulse produced when the same positrons dissipate their energy in the second crystal.

ii. Minton's method; that of using the 1.28 Mev. cascade gamma of Ne^{22} (the daughter product of Na^{22}) to determine the zero of time of the coincidence system, with the prompt curve being obtained by using a Co^{60} source together with side-channel energy selection.

iii. The present method; similar to Minton's, except that an "artificial" Na^{22} source is used, namely As^{76}, to obtain the prompt resolution curve.

The similarity of the results for the first and last methods outlined above suggests that the effect of gamma-ray energy on centroid shifts was not sufficiently corrected for in Minton's measurements.

It is also important to note that, since the 1.21 Mev. gamma ray of As^{76} precedes the 560 Kev. gamma, the lifetime

quoted in this experiment for the annihilation of positrons in aluminium, is actually 1.6×10^{-10} sec. + τ_{560}, where τ_{560} is the lifetime of the first excited state of Se^{76}. However, judging from the narrowness of the prompt resolution curve as compared to the aluminium absorber curve, the assumption that the lifetime of this excited state is much shorter than the lifetime of positrons in aluminium seems justified.

It thus appears that the lifetime of positrons in metals is indeed about 1.5×10^{-10} sec. rather than a factor of four larger as expected from the rapid conversion hypothesis (Garwin 1953). Therefore it seems that one is forced either to admit of a process for the formation of positronium only in the singlet state without the accompaniment of rapid conversion or to assume that the conversion process is irreversible, that is, the ortho-para conversion is highly probable, while the para-ortho is not. At present, however, the theoretical explanation of such a process is difficult (Garwin 1953), since there is very little energy difference between the triplet and singlet states of positronium.

Before a complete explanation of the positron annihilation process in metals can be given, there will probably be a need for more knowledge concerning the dependence of the small lifetime variations (Bell and Graham 1953), of positrons in metals as a function of the physical characteristics of the metals, like Atomic Number and Fermi energies, and also the

various environmental conditions (temperature, magnetization, etc.). For the above projects, equipment with greater stability, less experimental error, and better resolution will be required than that which has been used in the past. An improved fast time-sorter, based on the type described in this thesis, might well be a suitable tool for these studies.

APPENDIX A

THE DERIVATION OF A THEORETICAL COINCIDENCE RESOLUTION CURVE

I. For a Parallel Coincidence Circuit.

1. Assumptions:

(i) The probability of emission of the first photo-electron from the cathode of the photo-multiplier tube at a time between t and t+dt after the interaction of a gamma ray with the scintillator is given by:

$\frac{1}{\bar{t}} e^{-\frac{t}{\bar{t}}}$, where $\bar{t}$ is the mean time delay of the first photo-electron (Post and Schiff 1950)

(ii) The spread in electron transit time in the photo-multiplier tube is sufficiently small, that its effect on the probability distribution of (i) is negligible (Bell et al. 1952).

2. Derivation:

Let the probability of an output pulse from the counter occurring between time t and t+dt after the interaction of a gamma ray with the scintillator be:

(1) $p(t)dt = se^{-st}dt$, where $s = 1/\bar{t}$.

The constant transit time of the current pulse in the photo-multiplier tube is neglected in this discussion, since its effect is merely a translation of the origin.

The following figure will facilitate the discussion

of the resolution time. Zero time is the time of arrival of the coincident gamma rays at the counters.

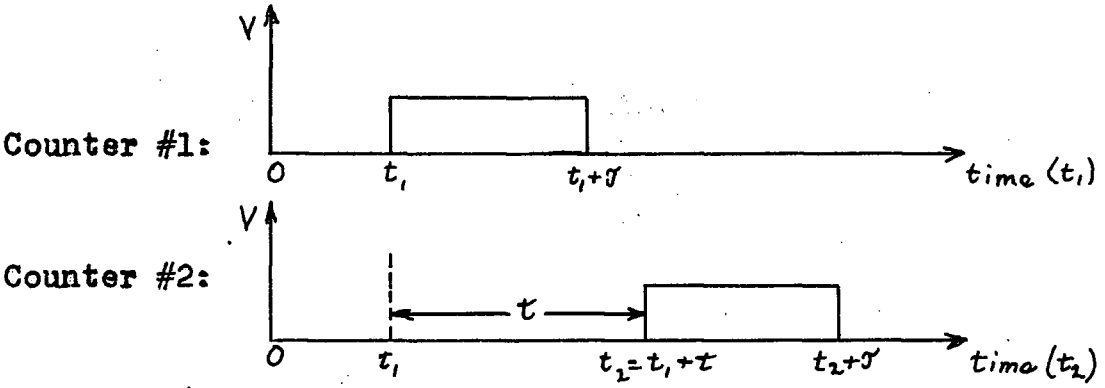

τ is the length of the equalized pulse determined by the shorting-stub length. If t is a time delay inserted into counter 1, then: an output pulse will be produced by the coincidence detector, if the pulse from counter #2 follows that from counter #1 by a time between $t-\tau$ and $t+\tau$.

Therefore the total probability of the recording of a coincidence when a delay of length t is inserted in counter #1, is the integral over all t_1 of the product of:
(A), the probability of a pulse from counter #2 in the time interval $t_1+t-\tau$ to $t_1+t+\tau$, and,
(B), the probability of a pulse from counter #1 at a time t. (Given by equation (1))

(A) the probability of a pulse from counter #2 in the time interval $t_1+t-\tau$ to $t_1+t+\tau$ is:

$$(2)\qquad p(t+t_1) = \int_{t_1+t-\tau}^{t_1+t+\tau} s e^{-st_2}\,dt_2 = e^{-s(t+t_1-\tau)} - e^{-s(t+t_1+\tau)}, \quad \text{for } t_1 \geq \tau - t, (t_2 \geq 0),$$

$$(3)\quad \text{and } p(t+t_1) = \int_{0}^{t_1+t+\tau} s e^{-st_2}\,dt_2 = 1 - e^{-s(t+t_1+\tau)}, \quad \text{for } t_1 \leq \tau - t.$$

Before forming the product probability and integrating, it

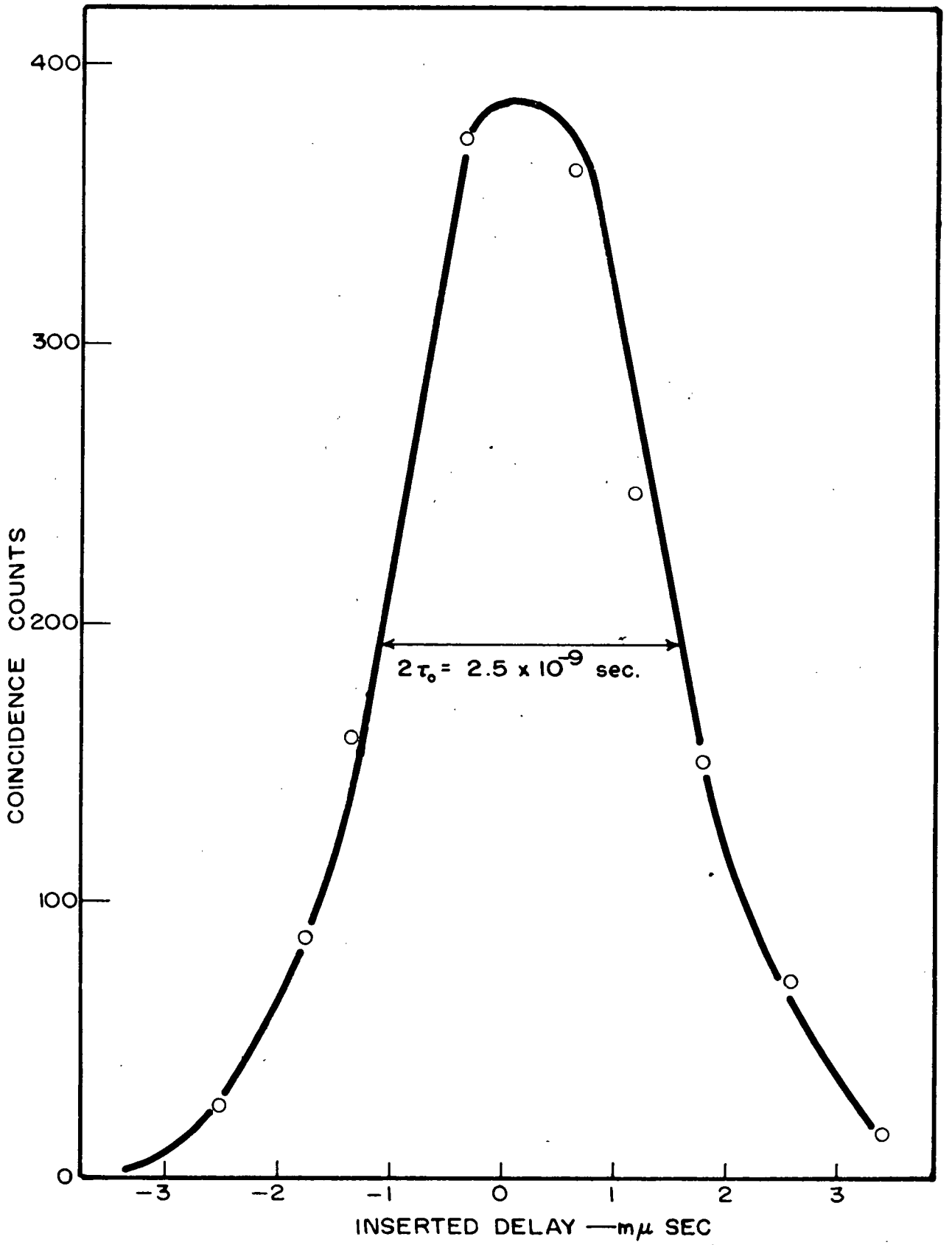

FIGURE 24: COINCIDENCE RESOLUTION CURVE FOR PARALLEL COINCIDENCE CIRCUIT
Theoretical Curve Fitted to Experimental Points

is convenient to distinguish between two cases:

1. The inserted delay $t \geq \tau$,

and 2. $t \leq \tau$.

Case 1: If $t \geq \tau$, then t_1 is necessarily $\geq \tau - t$, since $t_1 \geq 0$.

$\therefore$ P(t), the integral of the product probability,

$$= \int_0^\infty s\left[e^{-s(t_1+t-\tau)} - e^{-s(t_1+t+\tau)}\right]e^{-st_1}\,dt_1$$

$$= \sinh s\tau e^{-st}. \tag{4}$$

Case 2: If $t \leq \tau$, then the integration over t_1 must be carried out in two parts, depending on whether t_1 is greater than or less than $\tau - t$. (See equation (2) and (3) above.)

$$\text{i.e. } P(t) = \int_0^{\tau-t} s\left[1 - e^{-s(t_1+t+\tau)}\right]e^{-st_1}\,dt_1 + \int_{\tau-t}^\infty s\left[e^{-s(t+t_1-\tau)} - e^{-s(t+t_1+\tau)}\right]e^{-st_1}\,dt_1$$

$$= 1 - e^{-s\tau}\cosh st. \tag{5}$$

The same expressions are obtained if we consider the insertion of delay in counter #2 instead of counter #1.

Thus, the theoretical distribution is given by:

$$P(t) = 1 - e^{-s\tau}\cosh st, \qquad |t| \leq \tau,$$

$$= \sinh s\tau e^{-s|t|}, \qquad |t| \geq \tau.$$

This is fitted to an experimental curve in Fig. 24, with the following values being assigned to the parameters:

$$\tau = 1.25 \times 10^{-9}\ \text{sec.}$$

$$s = \frac{1}{\bar{t}} = \frac{1}{0.71 \times 10^{-9}\ \text{sec.}}$$

3. Conclusions:

(i) As $t \to 0$, $P(t) \to 1-e^{-s\tau}$, not $(1-e^{-s\tau})^2$ as assumed by Bell et al. (1952). A coincidence efficience of 90% (90% probability of detection of coincident pulses when t=0) is obtained with $2\tau = 4.6\,\bar{t}$, rather than $6\bar{t}$ as given by Bell et al (1952). A 95% coincidence efficiency is given by $2\tau = 6\bar{t}$.

(ii) The resolving time or "effective width," $2\tau_o$, of a coincidence resolution curve, is defined as the area under the curve divided by the maximum height (Bell et al. 1952).

$$\text{Area under curve} = 2\int_0^\infty P(t)\,dt = 2\tau.$$

$$\text{Maximum height} = 1-e^{-s\tau}.$$

$$\therefore\ 2\tau_o = \frac{2\tau}{1-e^{-s\tau}},$$ which is close to 2τ for $\tau > \bar{t}$, and is within 90% of 2τ for $\tau > 2.5\,\bar{t}$.

(iii) The relation between 2τ and the full width of the resolution curve at half maximum, $2t_{\frac{1}{2}}$: can readily be calculated:

$$P(t_{\frac{1}{2}}) = \sinh s\tau\, e^{-st_{\frac{1}{2}}}$$

$$P(0) = 1-e^{-s\tau}$$

$$\therefore \frac{P(t_{\frac{1}{2}})}{P(0)} = \frac{1}{2} = \frac{\sinh s\tau\, e^{-st_{\frac{1}{2}}}}{1-e^{-s\tau}}$$

$$\text{or: } e^{s\tau} = e^{st_{\frac{1}{2}}} - 1$$

$t_{\frac{1}{2}}$ is therefore somewhat greater than τ, but is less than 1.1τ for $\tau > 2\bar{t}$.

II. For a Time-Sorter.

1. Assumptions: In addition to the assumptions of part I, we assume:

(i) The time-sorter output pulse amplitude is proportional to the degree of overlap of the input pulse.

(ii) A fixed delay of time T is inserted into counter #2 so as to obtain a pulse overlap of about 1/2 for prompt pulses. This has the effect in the following discussion, of always causing the counter #1 pulse to arrive first at the detector.

The equalized pulse length (about 2T) is assumed to be much longer than the time resolution of the instrument. Let t be the time interval between the production of pulses by counter 1 and counter 2 from a coincidence event. We are interested in the amplitude spectrum of the pulses from the time-sorter resulting from the natural variations in this time t.

2. Derivation:

The probability of a pulse from counter #2 occurring between time

(6) t_1+t and $t_1+t+dt = se^{-s(t_1+t)}dt$.

Therefore the total probability of a pulse amplitude output corresponding to an overlap of T-t, to T-t-dt, is the integral over all values of t_1, of the product of the probability functions (1) and (6).

(7) i.e. $P(t)dt = \int_0^\infty s^2 e^{-st_1} e^{-s(t_1+t)} dt_1 = \frac{1}{2} s e^{-st} dt.$

Again, the same equation is the result of assuming that the counter #1 pulse is delayed by t. Thus, absolute values of t are used.

Actually, the amplitude measuring device (a pulse height analyzer) has a finite resolution determined by the channel width. Let the corresponding time-width of a channel be 2τ.

Then the probability of coincident pulses being observed in channel "t," is given by the integral of (7) from $t-\tau$ to $t+\tau$.

i.e. $$P_t = \int_{t-\tau}^{t+\tau} \tfrac{1}{2} s e^{-s|t|} dt = \sinh s\tau \, e^{-s|t|}, \quad \text{for } |t| \geq \tau$$

and $$= \int_0^{t+\tau} \tfrac{1}{2} s e^{-s|t|} dt + \int_0^{\tau-t} \tfrac{1}{2} s e^{-st} dt, \quad \text{for } |t| \leq \tau:$$

integrating over the peak of the curve;

$$= 1 - e^{-s\tau} \cosh st.$$

Since 2τ is the width of a channel, this latter function will apply only to:

a. the centre channel, if the peak is centred.

b. the centre two channels if the peak is split.

3. Conclusions

(i) The resulting formulae are identical with those arising from the parallel coincidence circuit, with the kick-sorter channel width now playing the role of the equalized pulse length of the parallel coincidence circuit.

(ii) These formulae were derived from the case where t can approach infinity: therefore the standardized pulse length must be much greater than t, to ensure essentially 100% coincidence efficiency.

(iv) Since the resulting formulae for the time-sorter are the same as those for the coincidence circuit, the considerations for effective width, half width, etc., which were obtained for the coincidence circuit, also apply in this case.

APPENDIX B

IMPEDANCE MISMATCHES

Fuchs (1952) gives the following formula for the reflectivity (ρ) of a short impedance discontinuity:

$\rho = \frac{2T}{t_r} \cdot \frac{Z_o' - Z_o}{Z_o' + Z_o}$, where T is the transit time of the pulse along the discontinuous impedance Z_o',

t_r is the rise time of the pulse,

and Z_o is the characteristic impedance of the cable.

For a 50 ohm, Amphenol connector, of length 2.75 cm.,

$$T = \frac{2.75}{3 \times 10^{10}} = 0.92 \times 10^{-10} \text{ sec.}$$

Assuming: $t_r \lesssim 0.5 \times 10^{-9}$ sec. (since the slope of the resolution curve indicates a rise time of about 3×10^{-10} sec.)

$Z_o = 100\,\Omega$, and $Z_o' = 50\,\Omega$,

$$\rho = \frac{2 \times .92 \times 10^{-10}}{.5 \times 10^{-9}} \times \frac{50}{150} = 0.12$$

Thus a transmission of better than 88% is obtained for the fast pulse.

APPENDIX C

CENTROID SHIFT METHOD OF CALCULATING SHORT HALF-LIVES

Bell et al. (1952) state that "the centroid of F(t), the delayed resolution curve, is displaced positively along the time axis from the centroid of P(t), the prompt resolution curve, by an amount $= 1/\lambda$, the mean life of the delayed radiation, as first shown by Bay (1951)".

This result may be simply deduced from Newton's formula: (1950):

$$\frac{dF}{dt} = \lambda(P-F).$$

By multiplying both sides by tdt and integrating, we obtain :

$$\lambda\left\{\int_{-\infty}^{\infty} t\,P\,dt - \int_{-\infty}^{\infty} t\,F\,dt\right\} = t\bar{F}\Big]_{-\infty}^{\infty} - \int_{-\infty}^{\infty} F\,dt$$

$$= -1.$$

$$\therefore \frac{1}{\lambda} = \mu_F - \mu_P,$$ where the symbol μ is used to denote centroid.

BIBLIOGRAPHY

Ajzenberg, F. and Lauritsen, T. (1955), Rev. Mod. Phys. 27, 77.

Bay, Z., (1951, Rev. Sci. Instr. 22, 397.

Bell, R.E., Graham, R.L., and Petch, H.E., (1952), Can. Journ. Phys. 30, 35.

Bell, R.E. and Graham, R.L. (1953), Phys. Rev. 90, 644.

Bell, R.E. (1954), Ann. Rev. of Nuclear Sci. 4, 93.

Benedict, M., (1937), Rev. Sci. Instr. 8, 252.

Bothe, W., (1930), Z. Physik, 59, 1.

De Benedetti, S., and Corben, H.C. (1954), Ann. Rev. of Nuclear Sci. 4, 191, contains an extensive bibliography.

De Benedetti, S., Cowan, C.E., Konneker, W.R., and Primakoff, H., (1950), Phys. Rev. 77, 205.

De Benedetti, S. and Richings, H.J. (1952), Phys. Rev. 85, 377.

De Benedetti, S., and Siegel, R.T., (1954), Phys. Rev. 94, 955.

Deutsch, M. (1948), Nucleonics, 2 (3), 58.

Deutsch, M., (1951), Phys. Rev. 82, 455.

Deutsch, M., (1951), Phys. Rev. 83, 866.

Dixon, W.R. and Trainor, L.E.H. (1955), Phys. Rev. 97, 733.

Ferrell, R.A. (1955), A.P.S. Bull. 30, 5, 27A.

Fischer, J., and Marshall, J. (1952), Rev. Sci. Instr. 23, 417.

Fuchs, G. (1952), Proc. Instn. Elect. Engrs. (April), 1952, Part iv.

Garwin, R.L., (1953), Phys. Rev. 91, 1571.

Green, R.E., and Stewart, A.T. (1955), Phys. Rev. 98, 486.

Heitler, W. (1954), "The Quantum Theory of Radiation," (Clarendon Press, Oxford, 1954).

BIBLIOGRAPHY

Hubert, P. (1953), Ann. de Phys. 8, 695.

Kallmann, H., (1947), Natur. u. Tech., July, 1947,

Lang, G., De Benedetti, S. and Smoluchowski, R. (1955), Phys. Rev. 99, 596.

Lee-Whiting, G.E. (1955), Phys. Rev. 97, 1557.

Lewis, I.A.D. and Wells, F.H. (1954), "Millimicrosecond Pulse Techniques," (London, Pergammon Press, 1954).

Mackenzie, I.K. (1953), Unpublished PhD. Thesis, The University of British Columbia.

Meyer, K.P., Baldinger, E., and Huber, P. (1948), Rev. Sci. Instr. 19, 473.

Millett, W.E. (1951), Phys. Rev. 82, 336.

Minton, T.D. (1950), Phys. Rev. 78, 490.

Neilson, G.C., and James, D.B. (1955), to be published, Rev. Sci. Instr., 1955.

Newton, T.D. (1950), Phys. Rev. 78, 490.

Ore, A. and Powell, J.L. (1949), Phys. Rev. 75, 1696.

Pirenne, J. (1947), Arch. Sc. et Nat. 29, 257.

Post, R.F., and Schiff, L. (1950), Phys. Rev. 80, 1113.

Rich, J.A. (1951), Phys. Rev. 81, 140.

Ruark, A.E. (1945), Phys. Rev. 68, 278.

Segré, E. (1953), "Experimental Nuclear Physics," (John Wiley and Sons, Inc., N. York), Vol. II, 1953.

Stewart, A.T. (1955), Private Communication.

Wheeler, J.A. (1946), Ann. N.Y. Acad. Sc. 48, 219.